# THE CALIBRATION OF A COLLECTION MEDIUM FOR THE DETERMINATION OF PARTICLE VELOCITY

PROJECT THOR TECHNICAL REPORT No. 50

JULY 1962

Ballistic Analysis Laboratory
Institute for Cooperative Research
The Johns Hopkins University
3506 Greenway
Baltimore 18, Maryland

Contract DA-36-034-ORD-29RD
Philadelphia Ordnance District

Ordnance Research and Development Project No. TB3-0238
Department of the Army Project No. DA5B03-05-010

Ballistic Research Laboratories
Aberdeen Proving Ground, Maryland

TABLE OF CONTENTS

LIST OF TABLES

LIST OF FIGURES

LIST OF FIGURES (CONT)

ABSTRACT

Previous investigations dealing with efforts to calibrate various media for the determination of particle velocity were usually restricted to steel particles impacting at normal obliquity with velocities up to 4000 feet per second. The present report provides a useful calibration of a medium for estimating particle velocities over a broad range of particle sizes, velocities, materials, and obliquities of strike.

Compact fragments of plastic, magnesium alloy, aluminum alloy, steel, and tungsten alloy have been used in single-fragment firings on a particular variety of fiberboard at the Ballistic Research Laboratories to produce the needed experimental data. A single empirical formula has been fitted to the data, relating striking velocity to the impact parameters of thickness of medium penetrated, angle of obliquity of strike, particle size, and presented area.

An effort has also been made to determine limiting impact conditions for each fragment material for which the fragment will remain essentially intact during the penetration. Whenever the fragment breaks up or deforms excessively during the penetration, the velocity estimates are no longer valid.

# INTRODUCTION

For several years, this laboratory has been participating in programs sponsored by the Weapon Systems Laboratory, Ballistic Research Laboratories (BRL), to supply information for vulnerability analysts and weapons designers on the resistance of various materials to perforation by fragments and projectiles. The bulk of the experimental data has been provided by BRL. Several reports have been published on the analyses of such data; the identification of these reports is given in Table I.

The present report describes a method for estimating the velocity of a particle on the basis of the extent of its penetration into an appropriate collecting medium.

The velocity of an isolated particle can be measured satisfactorily by any of several conventional techniques. The situation is complicated when several particles are moving together at different velocities. Such a situation is encountered, for example, when a target material is hit by a fragment and large numbers of particles of target material and fragment material issue forth from the back surface of the target material. By collecting these particles in a soft medium, it becomes possible to describe the weight, velocity, and spatial patterns or distributions of the particles. A knowledge of such characteristics leads to a more complete resolution of the effects of the initial impact.

In low velocity impacts the main result of the impact, when perforation is achieved, is usually one large particle of fragment origin. Several small particles of target origin may also be formed but their low velocity combined with their low mass suggest a negligible damage potential.

High velocity impacts are characterized by some break-up of the

TABLE I

Other Ballistic Analysis Laboratory Reports on Studies of the Perforation of Target Materials by Fragments and Projectiles

| Report No. | Date | Title | Classification |
|---|---|---|---|
| 14 | Sept. 1954 | A Suggested Technique for Predicting the Performance of Armor-Piercing Projectiles Acting on Rolled Homogeneous Armor (U) | C |
| 25 | July 1956 | A Comparison of Various Materials in Their Resistance to Performation by Steel Fragments; Empirical Relationships (U) | C |
| 36 | April 1958 | A Study of Residual Velocity Data for Steel Fragments Impacting on Four Materials; Empirical Relationships (U) | C |
| 41 | May 1959 | A Comparison of the Performance of Fragments of Four Materials Impacting on Various Plates (U) | C |
| 44 | Jan. 1960 | The Resistance of Two Nose-Cone Materials to Perforation by Steel Fragments; Empirical Relationships for Fragment Residual Velocity and Residual Weight (U) | S |
| 47 | April 1961 | The Resistance of Various Metallic Materials to Perforation by Steel Fragments; Empirical Relationships for Fragment Residual Velocity and Residual Weight (U) | C |

fragment on impact and the formation of many particles. Here, the damage potential of the particles formed from the impact can no longer be expressed in terms of the damage potential of a single particle. Furthermore, the particles are more numerous and several particles may have sufficient mass and velocity to warrant consideration as lethal agents.

Several materials have been tried out as collecting media. Some issues that are of importance in the choice of such materials are 1) availability, 2) cost, 3) quality control (product standardization), and 4) feasibility for experimental purpose. When a collecting medium stops a fast-moving particle, there is, inevitably, some abrasion, deformation, or even some disintegration of the particle. For laboratory purposes, the medium must offer sufficient resistance to the moving particle that it will stop the particle within a convenient thickness of the medium. Usually, the less dense the medium, the greater the thickness that is required to stop a given, moving particle. Some compromise is needed in the selection of the medium in regard to density and those characteristics of the medium which influence the effects on the particle during the penetration. Styrofoam, for example, is a low density material which appears to be capable of stopping particles with negligible effects on the particle shape and weight, but for particles of high velocity and/or large weight, the thickness required is prohibitive in many laboratory facilities for space reasons. On the other hand, soft metals like aluminum or magnesium might be considered, but even soft metals will punish the particle excessively during the "capture" of the particle.

Whenever the fragment deforms or breaks up appreciably during the penetration of the collecting medium, the fragment's performance deteriorates, i.e., the fragment does not penetrate the collecting medium as far as would

be expected on the basis of results of other impacts. The basic assumption in the determination of an empirical fit is that the faster a given particle, the deeper it will penetrate the collecting medium. To retain the validity of this assumption, it is therefore necessary to weed out from the data samples cases where the fragment has either deformed or broken up extensively.

## THE COLLECTING MEDIUM

Maftex was chosen as the collecting medium to be calibrated. It is a type of insulation board manufactured by MacAndrews and Forbes Co., Camden, New Jersey. The dimensions of standard production sheets are 4 feet by 8 feet by 1/2 inch. Thinner sheets of 5/16 inch are also available.

The approximate composition of this material is 40 to 50% plant root fiber (such as specially processed and defibrated licorice root), 30 to 40% coniferous wood fiber, 20 to 30% refined wood pulp, and sufficient asphalt to offer water resistance and strength.

Some physical characteristics of this material are a) moisture, 4 to 8%, b) density, 15 to 17 $lb/ft^3$, c) tensile strength, 200 to 300 $lb/in^2$, and d) absorption, 2 to 5% by volume.

Production sheets are cut into convenient sizes (usually 4 by 4 feet) and stacked for laboratory use. For a given impact condition, the pack is always thicker than necessary to halt the particle. After each firing, that portion of the pack which has not been damaged by the firing is removed for use in another pack.

Care should be exercised in the storage of Maftex so that the moisture content remains relatively constant.

## FRAGMENT MATERIALS AND TYPES

Cylindrical and spherical pre-formed fragments of five materials have been used in single-shot firings at BRL to produce the experimental data. The fragment materials chosen for the experimental work are Lexan, a magnesium alloy designated AZ31 B, aluminum alloy 2024T-4, steel, and Mallory 3000.

Lexan is a polycarbonate manufactured by General Electric. It has a density of about 75 $lb/ft^3$. Lexan is representative of several plastics which have been found useful for various Ordnance applications.

Magnesium alloy, aluminum alloy, and steel are typical structural materials in military targets. The densities are 113, 165, and 490 $lb/ft^3$, respectively.

Mallory 3000 is a tungsten alloy containing 7% iron and 3% nickel. It has a hardness of 24 on the Rockwell C scale. Its density is approximately 1061 $lb/ft^3$. High density materials are receiving much attention for certain military requirements.

When a structural material is struck by a fragment and the rear surface is damaged, particles of the target material emanate from the rear surface. These particles, in many cases, have a considerable capacity for damage in their own right.

These five fragment materials span a wide range in density. They represent several classes of materials which have some significance, directly or indirectly, for the consideration of military targets.

The weights, dimensions, and average presented areas (assuming random orientation in flight) of all fragments used in the experimental work are presented in Tables II-VI. A fragment shape factor, c, has been determined for each fragment material, by averaging the ratios of the average presented

area to the two-thirds power of the fragment weight for each fragment of that material. The constancy of the individual values of c within a target material is consistent with the comment, previously made, that the fragments were designed to be essentially homologous. Some fluctuation is expected since one must adapt the fragment designs to accommodate the gun facilities available.

Table II

Characteristics of Plastic Fragments

| Weight m (grains) | Shape | Radius (inches) | Length (inches) | Average Presented area A (sq. in.) | $c = \frac{A}{m^{2/3}}$ |
|---|---|---|---|---|---|
| 0.10 | cylinder | .0375 | .075 | .00663 | .03078 |
| 0.25 | cylinder | .0500 | .104 | .01210 | .03049 |
| 1 | cylinder | .0800 | .166 | .03091 | .03091 |
| 5 | cylinder | .1495 | .232 | .09194 | .03144 |
| 10 | cylinder | .1995 | .260 | .14399 | .03102 |
| 15 | cylinder | .1995 | .390 | .18473 | .03037 |
| 30 | cylinder | .2495 | .498 | .29295 | .03034 |
| 60 | cylinder | .2940 | .739 | .47705 | .03113 |
| 120 | cylinder | .3440 | 1.054 | .75541 | .03105 |

Average value of shape factor, c, is 0.0308

Table III

Characteristics of Magnesium Alloy Fragments

| Weight m (grains) | Shape | Radius (inches) | Length (inches) | Average Presented Area A (sq. in.) | $c = \frac{A}{m^{2/3}}$ |
|---|---|---|---|---|---|
| 0.10 | cylinder | .0325 | .066 | .00598 | .02776 |
| 0.25 | cylinder | .0450 | .086 | .01108 | .02792 |
| 1 | cylinder | .0750 | .124 | .02849 | .02849 |
| 5 | cylinder | .1165 | .256 | .08034 | .02748 |
| 10 | cylinder | .1495 | .312 | .12841 | .02767 |
| 15 | cylinder | .1995 | .263 | .18062 | .02970 |
| 30 | cylinder | .2495 | .335 | .28488 | .02951 |
| 60 | cylinder | .2740 | .485 | .39399 | .02571 |
| 120 | cylinder | .3445 | .705 | .67434 | .02772 |
| 240 | cylinder | .3445 | 1.410 | 1.05584 | .02734 |

Average value of shape factor, c, is 0.0279

Table IV

Characteristics of Aluminum Alloy Fragments

| Weight m (grains) | Shape | Radius (inches) | Length (inches) | Average Presented Area A (sq. in.) | $c = \frac{A}{m^{2/3}}$ |
|---|---|---|---|---|---|
| 0.10 | cylinder | .0315 | .053 | .00418 | .01941 |
| 0.25 | cylinder | .0390 | .078 | .00717 | .01807 |
| 1.0 | cylinder | .0625 | .122 | .01811 | .01811 |
| 5 | cylinder | .1165 | .176 | .05353 | .01831 |
| 10 | cylinder | .1165 | .351 | .08555 | .01843 |
| 15 | cylinder | .1495 | .320 | .11025 | .01812 |
| 30 | cylinder | .1995 | .359 | .17502 | .01813 |
| 60 | cylinder | .2495 | .459 | .27767 | .01811 |
| 120 | cylinder | .2935 | .663 | .44098 | .01812 |
| 240 | cylinder | .3445 | .962 | .70700 | .01830 |

Average value of shape factor, c, is 0.0183

Table V

Characteristics of Steel Fragments

| Weight m (grains) | Shape | Radius (inches) | Length (inches) | Average Presented Area A (sq. in.) | $c = \frac{A}{m^{2/3}}$ |
|---|---|---|---|---|---|
| .05 | cylinder | .016 | .032 | .0012 | .0088 |
| .10 | cylinder | .020 | .040 | .00186 | .0086 |
| .215 | sphere | .031 | ---- | .00302 | .00841 |
| .250 | cylinder | .028 | .054 | .00352 | .00887 |
| 0.825 | sphere | .047 | ---- | .00679 | .00772 |
| 1.0 | cylinder | .047 | .075 | .0090 | .0090 |
| 2 | sphere | .062 | ---- | .01227 | .00773 |
| 5 | cylinder | .075 | .145 | .0257 | .0088 |
| 6.75 | sphere | .094 | ---- | .02761 | .00773 |
| 10 | cylinder | .075 | .290 | .0427 | .0092 |
| 15 | cylinder | .117 | .180 | .0549 | .0090 |
| 30 | cylinder | .150 | .213 | .0852 | .0088 |
| 60 | cylinder | .200 | .243 | .1388 | .0091 |
| 120 | cylinder | .250 | .313 | .2206 | .0091 |
| 240 | cylinder | .294 | .450 | .3430 | .0089 |
| 475 | cylinder | .345 | .659 | .5433 | .0087 |

Average value of shape factor, c, is 0.0088

Table VI

Characteristics of Tungsten Alloy Fragments

| Weight m (grains) | Shape | Radius (inches) | Length (inches) | Average Presented Area A (sq. in.) | $c = \frac{A}{m^{2/3}}$ |
|---|---|---|---|---|---|
| 0.10 | cylinder | .016 | .029 | .0011 | .0051 |
| 0.25 | cylinder | .021 | .042 | .0021 | .0053 |
| 1.00 | cylinder | .040 | .051 | .0057 | .0057 |
| 5.00 | cylinder | .063 | .094 | .0155 | .0053 |
| 10 | cylinder | .0745 | .134 | .0244 | .00526 |
| 15 | cylinder | .0745 | .201 | .0322 | .0053 |
| 30 | cylinder | .1165 | .162 | .0510 | .00528 |
| 60 | cylinder | .1495 | .199 | .0819 | .00534 |
| 120 | cylinder | .1995 | .225 | .1321 | .00543 |
| 240 | cylinder | .2495 | .287 | .2099 | .00544 |

Average value of shape factor, c, is 0.0054

## EMPIRICAL RELATIONSHIPS

A single empirical equation of the form

$$V = k\, e^{\alpha}\, m^{\beta}\, (\sec \theta)^{\gamma}\, A^{\lambda}$$

was selected to fit the experimental data for all the fragment materials. In this equation,

V is the fragment striking velocity in fps,

e is the thickness in inches of Maftex penetrated, measured along the normal to the surface of the Maftex,

m is the weight of the fragment in grains,

$\theta$ is the angle between the trajectory of the fragment and the normal to the surface of the Maftex,

A is the average presented area of the fragment in square inches, and

k, $\alpha$, $\beta$, $\gamma$ and $\lambda$ are constants determined for the equation by the Method of Least Squares,

The values of these constants which specify the equation are to be found in the Results Section.

The exponential form of this equation is simple, practical, and includes the vital impact parameters. The form has the additional merit of being convertible into a corresponding logarithmic form, useful for its linearity.

The goodness of fit of the estimating equation is given in terms of the values of $b'$ and $\sigma$, defined below. If $(\Delta V)_i$ is the difference between the experimental result and the formula prediction (in that order) for the i-th set of N sets of experimental conditions, then

$$b = \frac{\sum_{i=1}^{N} (\Delta V)_i}{N}$$

and

$$\sigma^2 = \frac{\sum_{i=1}^{N} (\Delta V)_i^2}{N}$$

It is understood that the final selection of the set of constants for the estimating equation is made to correspond with the lowest obtainable value of $\sigma$. It is also desirable for the value of b associated with the estimating equation to be close to zero.

The following method is employed to obtain an empirical formula for estimating particle velocity on the basis of depth of penetration into Maftex. The basic formula is converted into the associated logarithmic form:

$$\log V = \mu + \alpha \log e + \beta \log m + \gamma \log \sec \theta + \lambda \log A .$$

With this linear form, the method of least squares is employed to determine a satisfactory set of values $\mu$, $\alpha$, $\beta$, $\gamma$, and $\lambda$ which specify the logarithmic equation given above and the original, related equation as well.

Admittedly, this procedure minimizes S, defined below, rather than $\sigma$.

$$S^2 = \frac{\sum_{i=1}^{N} (\log V_i^* - \log V_i)^2}{N} .$$

Note that $V^*$ refers to the particle velocity as calculated by the formula, whereas V is the particle velocity determined experimentally for the same set of impact conditions.

The form of the estimating equation is but slightly different from the forms used in earlier reports.

The values of b and $\sigma$ for each fragment material are given in Table XII of the Summary Section. That section also contains a series of graphs showing for each fragment material the variations with velocity of the percentage of error in the velocity estimates.

The characteristics of the experimental data are shown in Appendix I.

## FRAGMENT DEFORMATION AND BREAK-UP

For each combination of fragment material and collecting medium, there seems to be a limit, probably expressible in terms of fragment velocity, below which the fragments remain essentially intact during the penetration of the medium. Above this limit, the fragment is likely to break up or deform to the extent that the fragment's performance becomes unpredictable.

To determine these limits, the fragments were recovered after impact on Maftex and examined for changes in shape and weight. A decision was given on the basis of a visual examination as to whether the fragment was essentially intact, moderately deformed, or seriously deformed. In addition, each recovered fragment was weighed to determine the loss in weight during the penetration of the medium. From these results it appears that a velocity can be established for each fragment material, under which the fragment (independent of its size) can be expected to penetrate Maftex with negligible effects on its shape and weight. These velocities are presented in the following chart.

| Fragment Material | Maximum Velocity |
|---|---|
| Plastic | 4200 |
| Magnesium Alloy | 5500 |
| Aluminum Alloy | 8500 |
| Steel | 10000 |
| Tungsten Alloy | 8000 |

Tables and graphs follow to sustain the selection of these velocities as cut-offs beyond which the velocity estimates as determined from the master estimating equation are probably unreliable since the collecting medium, Maftex, is expected to damage the fragment.

For higher velocities, the calibration of a softer collecting medium such as styrofoam might be useful. It is presumed that with any collecting medium, if the velocities are sufficiently high, the fragment will deform or break up during the penetration. Maftex appears to be a satisfactory medium for metallic fragment materials as long as the striking velocity is actually less than 5000 fps. For fragment materials of high tensile strength such as steel, it appears that velocities up to 10000 fps can be tolerated with this technique.

Table VII

Observations of Recovered Plastic Fragments After

Penetration of Maftex

| Striking Velocity (fps) | Fragment Essentially Intact | Fragment Moderately Deformed | Fragment Badly Deformed |
|---|---|---|---|
| < 2000 | ψ ψ ∂ ∂ ∂ * | | |
| 2000 to 3000 | Δ Δ ∂ ∂ | | |
| 3000 to 4000 | ψ ∂ * | Δ ψ ψ ψ | ∂ |
| 4000 to 5000 | * | ∂ | ψ |
| 5000 to 6000 | | | Δ ∂ ∂ ∂ * * |
| 6000 to 7000 | | | * |
| 7000 to 8000 | | | ∂ |
| 8000 to 9000 | | | |
| 9000 to 10000 | | | |
| > 10000 | | | |

Code

ø: $.01 \leq m < .10$

Δ: $.10 \leq m < 1.0$

ψ: $1.0 \leq m < 10$

∂: $10 \leq m < 100$

*: $100 \leq m < 10000$

m: fragment weight (grains)

Table VIII

Observations of Recovered Magnesium Alloy Fragments

After Penetration of Maftex

| Striking Velocity (fps) | Fragment Essentially Intact | Fragment Moderately Deformed | Fragment Badly Deformed |
|---|---|---|---|
| < 2000 | ψ ∂ ∂ * | | |
| 2000 to 3000 | Δ ψ * | | |
| 3000 to 4000 | Δ | | |
| 4000 to 5000 | ψ ψ ∂ ∂ ∂ | Δ | |
| 5000 to 6000 | * * | ψ ψ | |
| 6000 to 7000 | ∂ ∂ | | |
| 7000 to 8000 | | ∂ | ∂ |
| 8000 to 9000 | | | |
| 9000 to 10000 | | | |
| > 10000 | | | |

Code

ø: $.01 \leq m < .10$

Δ: $.10 \leq m < 1.0$

ψ: $1.0 \leq m < 10$

∂: $10 \leq m < 100$

*: $100 \leq m < 1000$

m: fragment weight (grains)

Table IX

Observations of Recovered Aluminum Alloy Fragments

After Penetration of Maftex

| Striking Velocity (fps) | Fragment Essentially Intact | Fragment Moderately Deformed | Fragment Badly Deformed |
|---|---|---|---|
| < 2000 | Δ Δ Δ ψ ψ ψ ψ ∂ | | |
| 2000 to 3000 | Δ Δ Δ Δ Δ ψ ψ ψ ψ ∂ | | |
| 3000 to 4000 | Δ Δ ψ ∂ ∂ ∂ | | |
| 4000 to 5000 | ∂ ∂ * | Δ | |
| 5000 to 6000 | | | |
| 6000 to 7000 | * | | |
| 7000 to 8000 | * | | ∂ |
| 8000 to 9000 | | | |
| 9000 to 10000 | | | ∂ |
| > 10000 | | | ∂ |

Code

ø: $.01 \leq m < .10$

Δ: $.10 \leq m < 1.0$

ψ: $1.0 \leq m < 10$

∂: $10 \leq m < 100$

*: $100 \leq m < 1000$

m: fragment weight (grains)

Table X

Observations of Recovered Steel Fragments After Penetration of Maftex

| Striking Velocity (fps) | Fragment Essentially Intact | Fragment Moderately Deformed | Fragment Badly Deformed |
|---|---|---|---|
| < 2000 | Δ Δ Δ Δ | | |
| 2000 to 3000 | ø Δ Δ Δ Δ | | |
| 3000 to 4000 | ø Δ Δ Δ Δ | | |
| 4000 to 5000 | ø | | |
| 5000 to 6000 | * | | |
| 6000 to 7000 | Δ * | | |
| 7000 to 8000 | Δ ∂ | | |
| 8000 to 9000 | | | |
| 9000 to 10000 | Δ | Δ Δ ∂ | |
| > 10000 | Δ Δ ∂ ∂ | | |

Code

ø: $.01 \leq m < .10$

Δ: $.10 \leq m < 1.0$

ψ: $1.0 \leq m < 10$

∂: $10 \leq m < 100$

*: $100 \leq m < 1000$

m: fragment weight (grains)

Table XI

Observations of Recovered Tungsten Alloy Fragments

After Penetration of Maftex

| Striking Velocity (fps) | Fragment Essentially Intact | Fragment Moderately Deformed | Fragment Badly Deformed |
|---|---|---|---|
| < 2000 | Δ ψ ψ ∂ | | |
| 2000 to 3000 | Δ Δ Δ ψ ψ ψ ∂ * | | |
| 3000 to 4000 | Δ Δ Δ Δ ψ ψ | | |
| 4000 to 5000 | Δ Δ ∂ * * | | |
| 5000 to 6000 | ψ ψ | | |
| 6000 to 7000 | Δ | | |
| 7000 to 8000 | Δ | | |
| 8000 to 9000 | | | |
| 9000 to 10000 | ∂ | ∂ ∂ | Δ |
| > 10000 | | ∂ ψ ψ | ψ |

Code

ø: $.01 \leq m < .10$

Δ: $.10 \leq m < 1.0$

ψ: $1.0 \leq m < 10$

∂: $10 \leq m < 100$

*: $100 \leq m < 1000$

m: fragment weight (grains)

## PERCENTAGE OF WEIGHT LOST DURING MAF TEX PENETRATION

Plastic Fragments

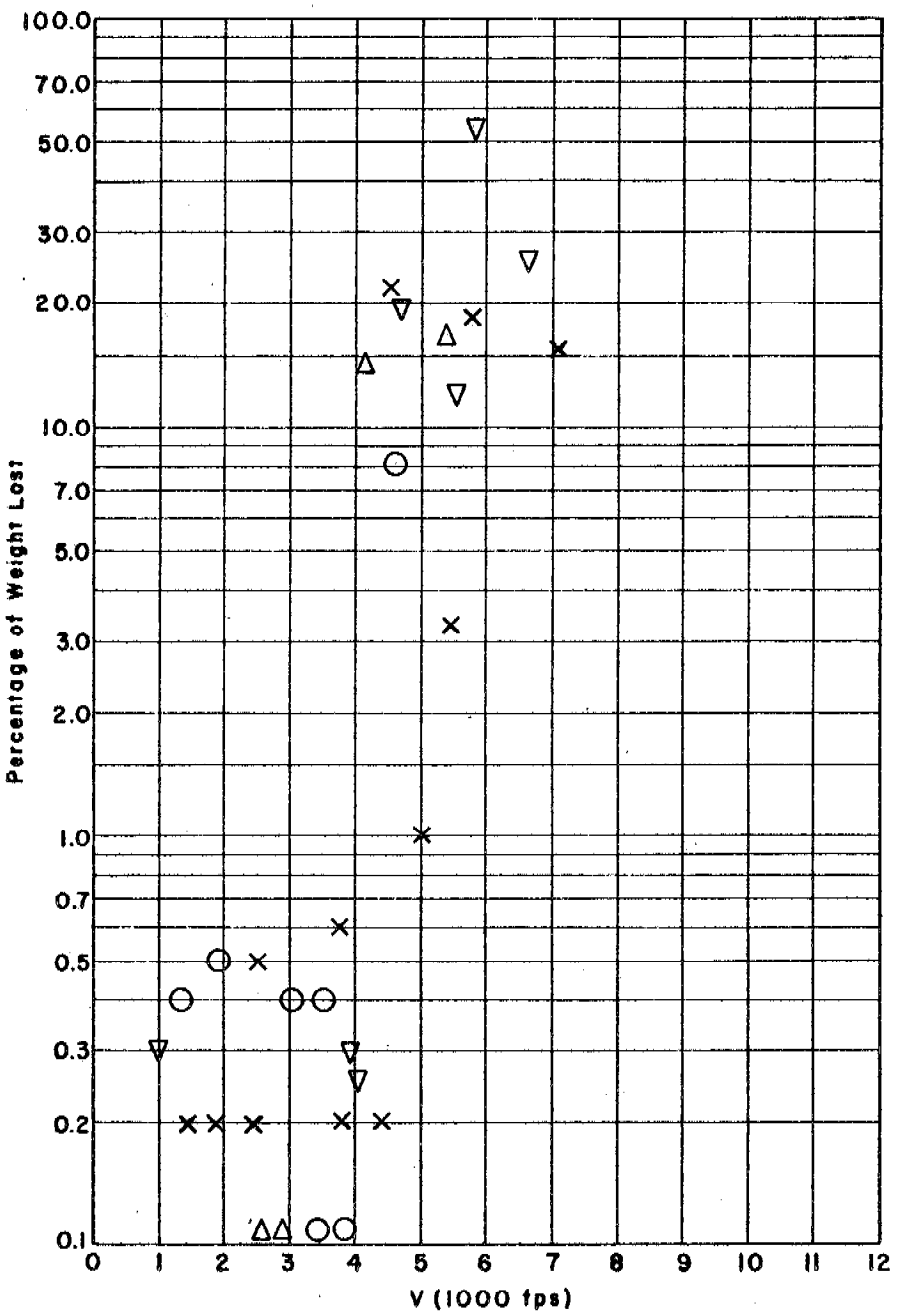


| LEGEND | | | | |
|---|---|---|---|---|
| + | | m < | 0.1 | |
| Δ | 0.1 ≤ | m < | 1.0 | |
| O | 1.0 ≤ | m < | 10.0 | |
| × | 10.0 ≤ | m < | 100.0 | |
| ∇ | 100.0 ≤ | m | | |

m: fragment weight (grains)

Fig. 1

PERCENTAGE OF WEIGHT LOST
DURING MAF TEX PENETRATION

Magnesium Alloy Fragments

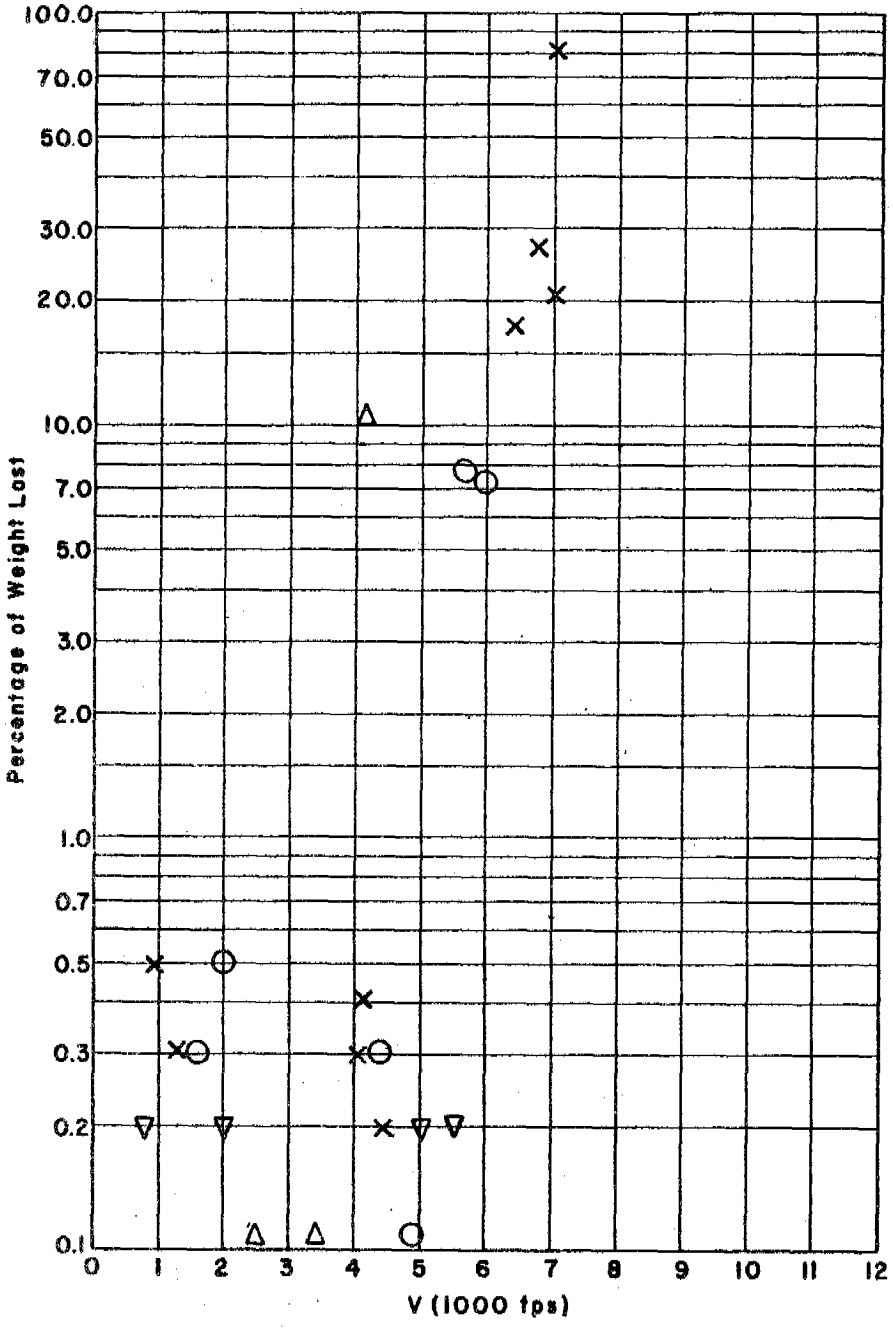


| LEGEND | | | | |
|---|---|---|---|---|
| + | | m < | 0.1 | |
| Δ | 0.1 ≤ | m < | 1.0 | |
| O | 1.0 ≤ | m < | 10.0 | |
| × | 10.0 ≤ | m < | 100.0 | |
| ∇ | 100.0 ≤ | m | | |

m: fragment weight (grains)

Fig. 2

PERCENTAGE OF WEIGHT LOST
DURING MAF TEX PENETRATION
Aluminum Alloy Fragments

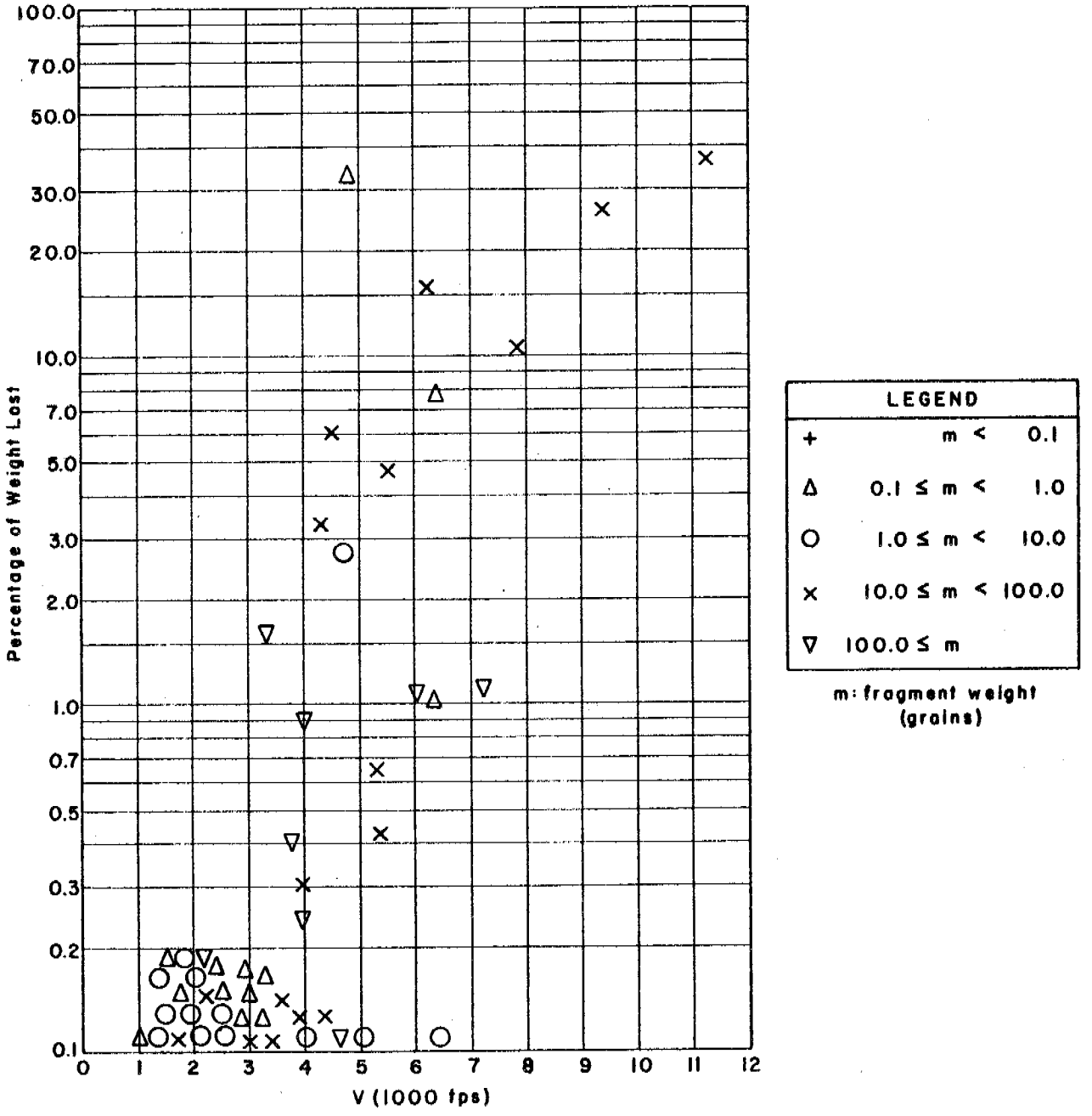


Fig. 3

PERCENTAGE OF WEIGHT LOST
DURING MAF TEX PENETRATION

Steel Fragments

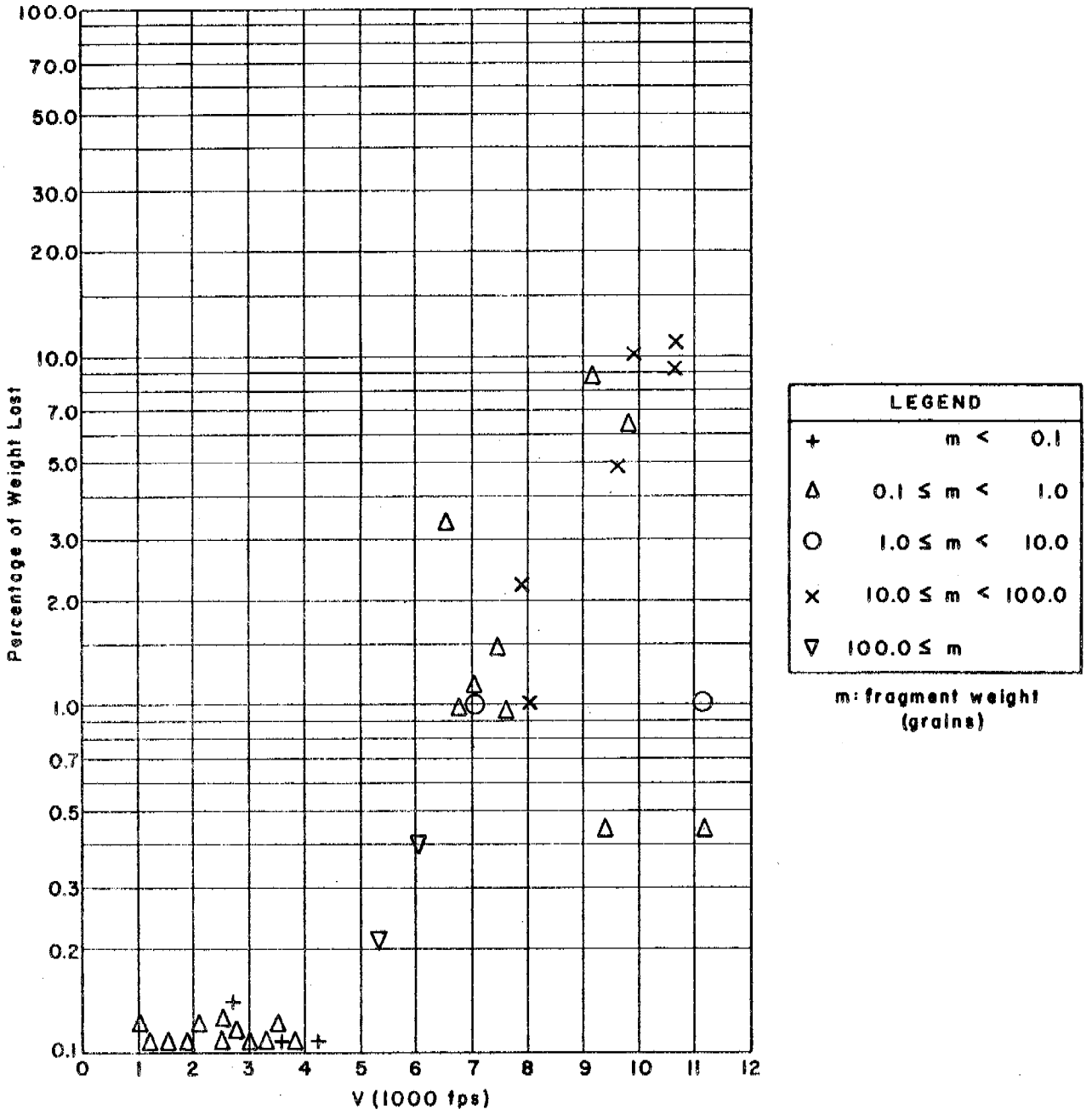


Fig. 4

PERCENTAGE OF WEIGHT LOST
DURING MAF TEX PENETRATION
Tungsten Alloy Fragments

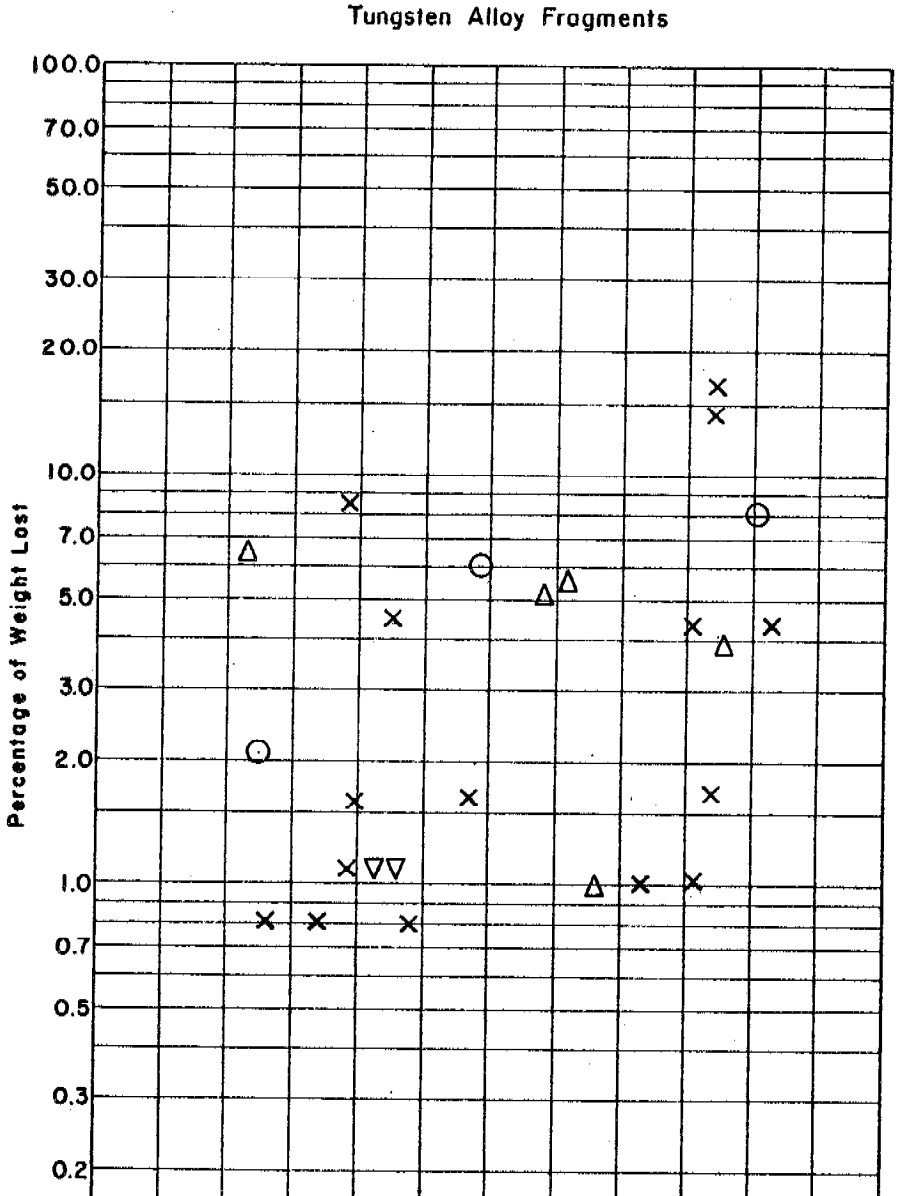


| LEGEND | | | | |
|---|---|---|---|---|
| + | | m < | 0.1 | |
| Δ | 0.1 ≤ | m < | 1.0 | |
| O | 1.0 ≤ | m < | 10.0 | |
| × | 10.0 ≤ | m < | 100.0 | |
| ∇ | 100.0 ≤ | m | | |

m: fragment weight (grains)

Fig. 5

## RESULTS

The master estimating equation relating striking velocity to other impact parameters for all five fragment materials is

$$V = 26170\ e^{0.736}\ m^{-0.681}(\sec\theta)^{0.711}\ A^{0.638}$$

where symbols and units are defined in the section, EMPIRICAL RELATIONSHIPS.

For each fragment material, a set of pre-formed fragments was designed to be essentially homologous, i.e., the same shape. For each material, it is possible to relate the average presented area of the fragment to the fragment weight by means of the equation: $A = cm^{2/3}$. The average value of c for each fragment material is given below:

| Fragment Material | c |
|---|---|
| Plastic | 0.0308 |
| Magnesium Alloy | 0.0279 |
| Aluminum Alloy | 0.0183 |
| Steel | 0.0088 |
| Tungsten Alloy | 0.0054 |

Note that with this type of formula, it is assumed that the difference in performances on Maftex between two fragments of the same weight and shape but of different materials can be accounted for by their different average presented areas. With the weight and shape of fragment fixed, the denser the material, the smaller the average presented area.

By substituting for A, in the master estimating equation, the appropriate function of m for each fragment material, a set of equations is generated.

$$\text{PLASTIC:} \quad V = 2838\, e^{0.736}\, m^{-0.255}\, (\sec\theta)^{0.711}$$

$$\text{MAGNESIUM ALLOY:} \quad V = 2664\, e^{0.736}\, m^{-0.255}\, (\sec\theta)^{0.711}$$

$$\text{ALUMINUM ALLOY:} \quad V = 2035\, e^{0.736}\, m^{-0.255}\, (\sec\theta)^{0.711}$$

$$\text{STEEL:} \quad V = 1276\, e^{0.736}\, m^{-0.255}\, (\sec\theta)^{0.711}$$

$$\text{TUNGSTEN ALLOY:} \quad V = 934\, e^{0.736}\, m^{-0.255}\, (\sec\theta)^{0.711}$$

Note that these equations vary only in the value of the coefficient. This suggests that the velocity estimate for each material can be given in terms of the velocity estimates for a selected material multiplied by some appropriate ratio or factor. If steel is selected as the standard, then the factor $f_V$, the ratio of the coefficient for the given material to that for steel, appears in the chart which follows.

By solving each equation in the previous set for e, another useful set of equations is generated.

$$\text{PLASTIC:} \quad e = 0.00002044\, m^{0.347}\, V^{1.358}\, (\cos\theta)^{0.966}$$

$$\text{MAGNESIUM ALLOY:} \quad e = 0.00002228\, m^{0.347}\, V^{1.358}\, (\cos\theta)^{0.966}$$

$$\text{ALUMINUM ALLOY:} \quad e = 0.00003211\, m^{0.347}\, V^{1.358}\, (\cos\theta)^{0.966}$$

$$\text{STEEL:} \quad e = 0.00006058\, m^{0.347}\, V^{1.358}\, (\cos\theta)^{0.966}$$

$$\text{TUNGSTEN ALLOY:} \quad e = 0.00009250\, m^{0.347}\, V^{1.358}\, (\cos\theta)^{0.966}$$

Again, one notes that the equations in this set vary only in the value of the coefficient. This suggests that the thickness of Maftex that would be penetrated by any fragment material can be given in terms of the thickness of Maftex that would be penetrated by, say, a steel fragment of the same weight, shape, velocity, and angle of obliquity of strike, multiplied by some appropriate factor or ratio. Steel, again, has been selected as the standard, and the factors $f_e$ appear (as well as those for $f_V$) in the chart below.

| $f_V$ | Fragment Material | $f_e$ |
|---|---|---|
| 2.23 | Plastic | 0.34 |
| 2.09 | Magnesium Alloy | 0.37 |
| 1.60 | Aluminum Alloy | 0.53 |
| 1.00 | Steel | 1.00 |
| 0.73 | Tungsten Alloy | 1.53 |

A set of five graphs follows, relating the impact parameters to each other. Each graph applies to a selected value of $\theta$, the angle of obliquity, between $0^\circ$ and $70^\circ$. Whereas these graphs are prepared for steel fragments, it will now be shown how they can be adapted for other fragment materials.

The graphs are useful for the solution of two types of problems. In the first problem, one is given e, m, $\theta$, for a compact fragment of material X. To find the velocity corresponding to these conditions, one determines the velocity for a compact steel particle of the same weight; then this result is multiplied by the factor $f_V$ corresponding to material X.

In the second problem, one is given V, m, $\theta$, for a compact fragment of material X. To find the thickness of Maftex that would be penetrated by such a fragment, one determines the thickness of Maftex that would be penetrated by a compact steel fragment of the same weight; then this result is multiplied by the factor $f_e$ corresponding to the material X.

The density range of the five fragment materials considered in the experimental work is so extensive that the master estimating equation can probably be useful in providing velocity estimates for other fragment materials as well. In Figure 6, the variation of the two sets of f values with fragment

density is shown. Accordingly, the reader can estimate the velocity of a particle of some material not actually under consideration in this report when the density of the material is known.

It should be remembered, however, that all the experimental work was executed with chunky fragments for which the ratio of maximum presented area to minimum presented area was never far removed from unity. Thus, the performance of fragments with the same characteristics do not fluctuate widely under the same firing conditions, providing the fragments are not breaking up or deforming while slowing down in the collecting medium.

In Figures 7-11 which follow, the inner rectangle delineates the conditions which represent the major effort of the experimental work. For example, few firings were made with fragments weighing less than 0.10 grains or with velocities in excess of 12,000 fps.

In using the equations or graphs to estimate particle velocity, the reader is cautioned that these results evolve from isolated or independent firings. One possible source of error is discussed. The user locates two particles in the same general region of the recovery medium, one large and one small. Not realizing that the smaller particle is a splinter particle of the larger one (and had therefore the same velocity on impact as the larger particle), the user might infer that the small particle had a velocity corresponding to that of a small particle which would independently penetrate that much of the collecting medium.

In the set of equations solved for e, the values of the exponents are remarkably close to 1/3, 4/3, and 1 respectively. This suggests that the equations might be adjusted to fit the form:

$$e \sec \theta = k'(mV^4)^{1/3}$$

where (e sec $\theta$) would represent the distance of travel through the Maftex pack along the line of travel. Of course, if there is some particular merit to this alternate form of the equation, one could return to the Least Squares technique and compute a best k' compatible with this form for the experimental data for each fragment material.

For a quick result, a sampling of sets of parameters (e, $\theta$, m, V) for steel fragments was made. The average value of k' where

$$k' = \frac{e \sec \theta}{(mV^4)^{1/3}}$$

corresponding to these sets was found to be 0.000080. If it is assumed that the same set of values for $f_e$ holds for this new form of equation, then a new set of equations of the form

$$e \sec \theta = k'(mV^4)^{1/3}$$

is generated where the value of k' for each fragment material is given in the following chart.

| Fragment Material | k' |
|---|---|
| Plastic | 0.000027 |
| Magnesium Alloy | 0.000029 |
| Aluminum Alloy | 0.000042 |
| Steel | 0.000080 |
| Tungsten Alloy | 0.000122 |

One ready advantage of the preceding form of the equation is the linearity of (e sec $\theta$) with $(mV^4)^{1/3}$. In Figure 12, a single graph displays the estimated variation of depth of Maftex penetration along the line of travel with this particular function of m and V. The ordinate has absorbed the obliquity factor.

The estimates of thickness of Maftex penetrated by a given fragment, as determined by this simplified equation and again as determined from the master estimating equation, are generally in excellent agreement.

For the reader's convenience, the principal set of graphs (Figures 7-11) shows two sets of units, grains and grams, on the abscissa axis and two sets of units, feet per second and meters per second, on the ordinate axis.

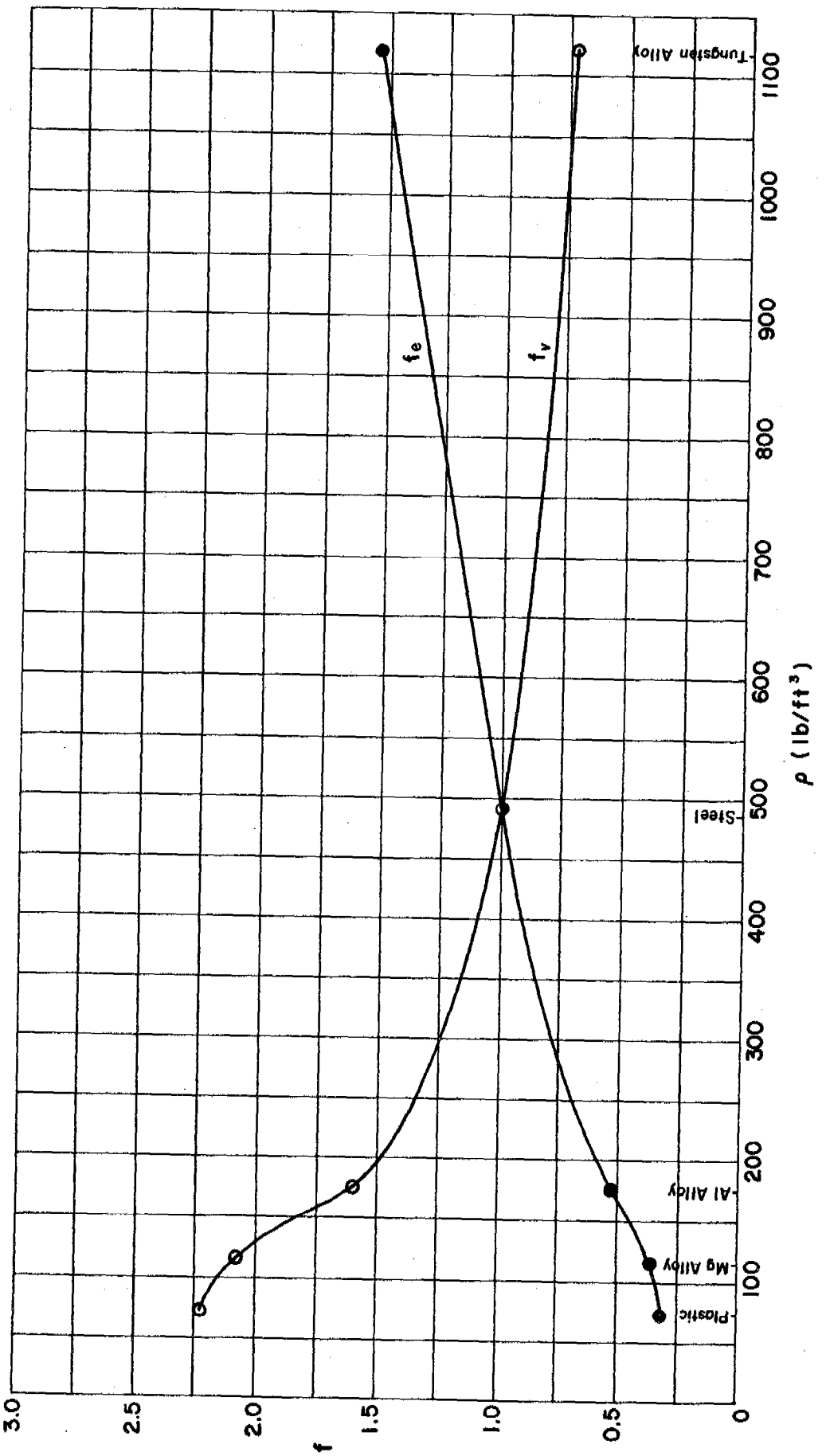
VARIATION OF f VALUES WITH FRAGMENT DENSITY
(Compact Fragments)
f
3.0
2.5
2.0
1.5
1.0
0.5
0
$f_e$
$f_v$
Plastic
Mg Alloy
Al Alloy
Steel
Tungsten Alloy
100
200
300
400
500
600
700
800
900
1000
1100
ρ (lb/ft³)

Fig. 6

## STEEL FRAGMENTS vs MAFTEX
## θ = 0°

| $f_v$ | Material | $f_e$ |
|---|---|---|
| 2.23 | Plastic | 0.34 |
| 2.09 | Mg Alloy | 0.37 |
| 1.60 | Al Alloy | 0.53 |
| 1.00 | Steel | 1.00 |
| 0.73 | Tungsten Alloy | 1.53 |

To obtain V for a fragment material other than steel, determine V for a steel particle, and multiply by the value of $f_v$ corresponding to the fragment material in question.

To obtain e for a fragment material other than steel, determine e for a steel particle, and multiply by the value of $f_e$ corresponding to the fragment material in question.

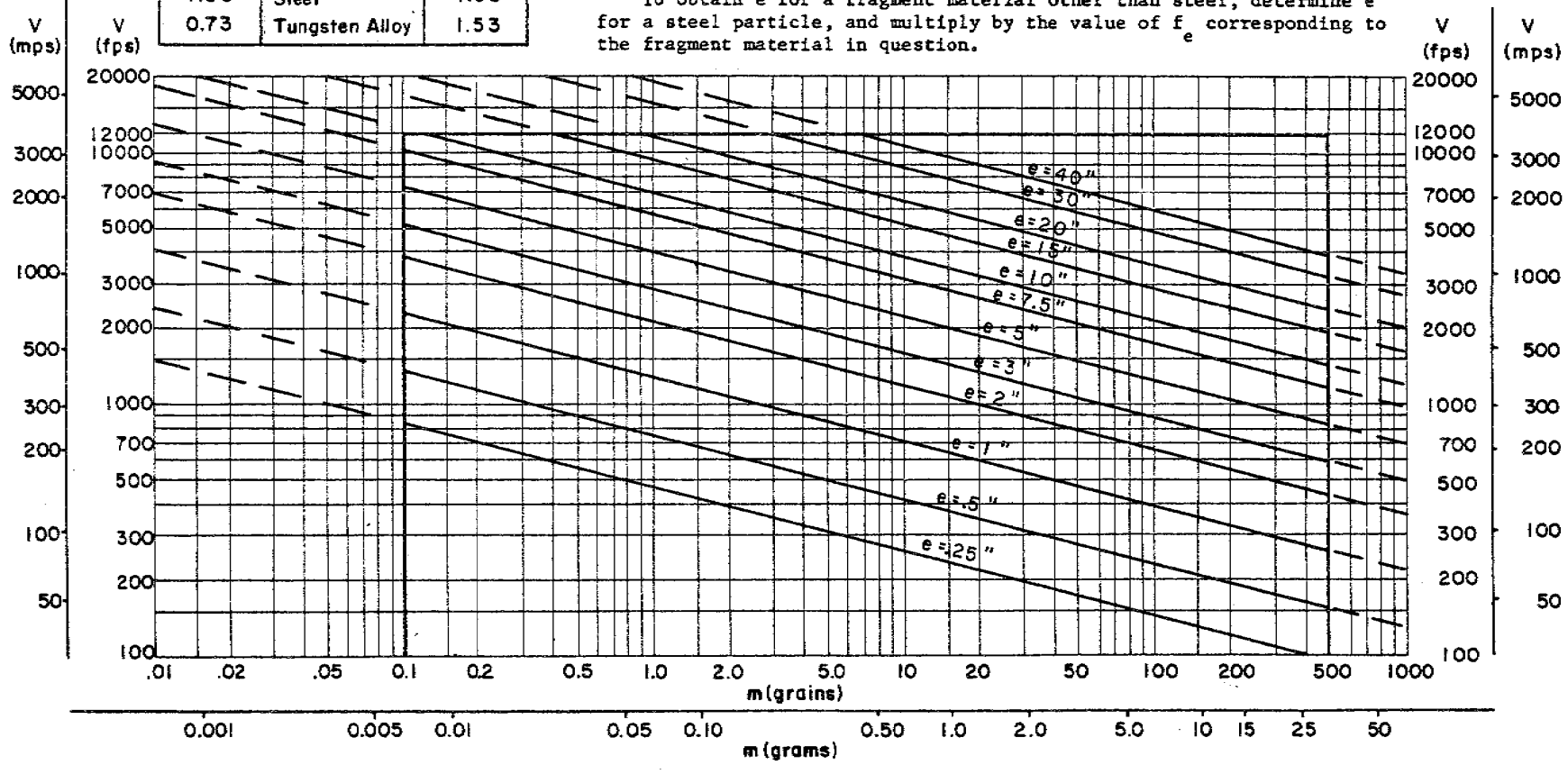


Fig. 7

## STEEL FRAGMENTS vs MAFTEX
## θ = 30°

| $f_v$ | Material | $f_e$ |
|---|---|---|
| 2.23 | Plastic | 0.34 |
| 2.09 | Mg Alloy | 0.37 |
| 1.60 | Al Alloy | 0.53 |
| 1.00 | Steel | 1.00 |
| 0.73 | Tungsten Alloy | 1.53 |

To obtain V for a fragment material other than steel, determine V for a steel particle, and multiply by the value of $f_v$ corresponding to the fragment material in question.

To obtain e for a fragment material other than steel, determine e for a steel particle, and multiply by the value of $f_e$ corresponding to the fragment material in question.

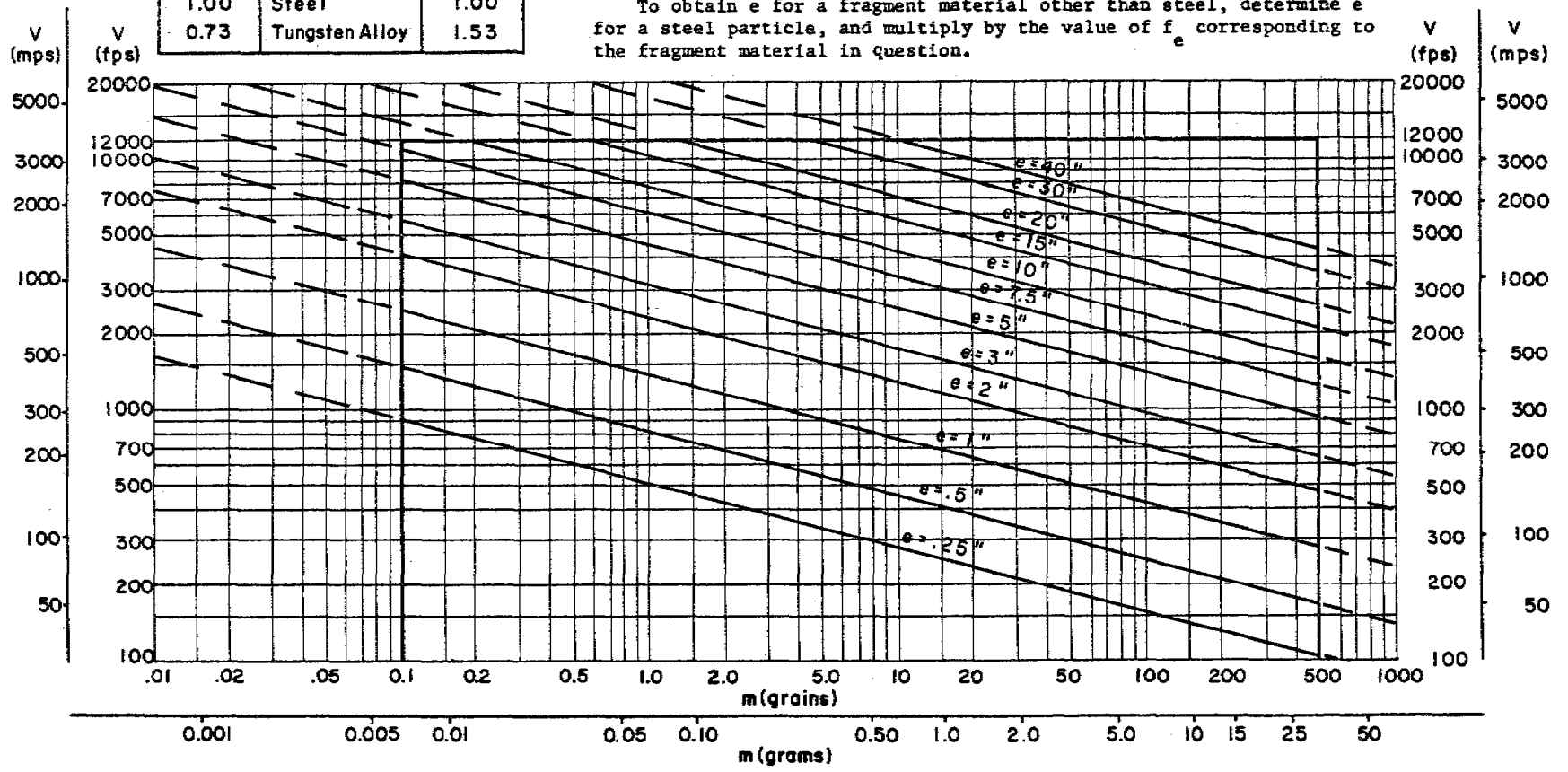


Fig. 8

| $f_v$ | Material | $f_e$ |
|---|---|---|
| 2.23 | Plastic | 0.34 |
| 2.09 | Mg Alloy | 0.37 |
| 1.60 | Al Alloy | 0.53 |
| 1.00 | Steel | 1.00 |
| 0.73 | Tungsten Alloy | 1.53 |

## STEEL FRAGMENTS vs MAFTEX
## $\theta = 45°$

To obtain V for a fragment material other than steel, determine V for a steel particle, and multiply by the value of $f_v$ corresponding to the fragment material in question.

To obtain e for a fragment material other than steel, determine e for a steel particle, and multiply by the value of $f_e$ corresponding to the fragment material in question.

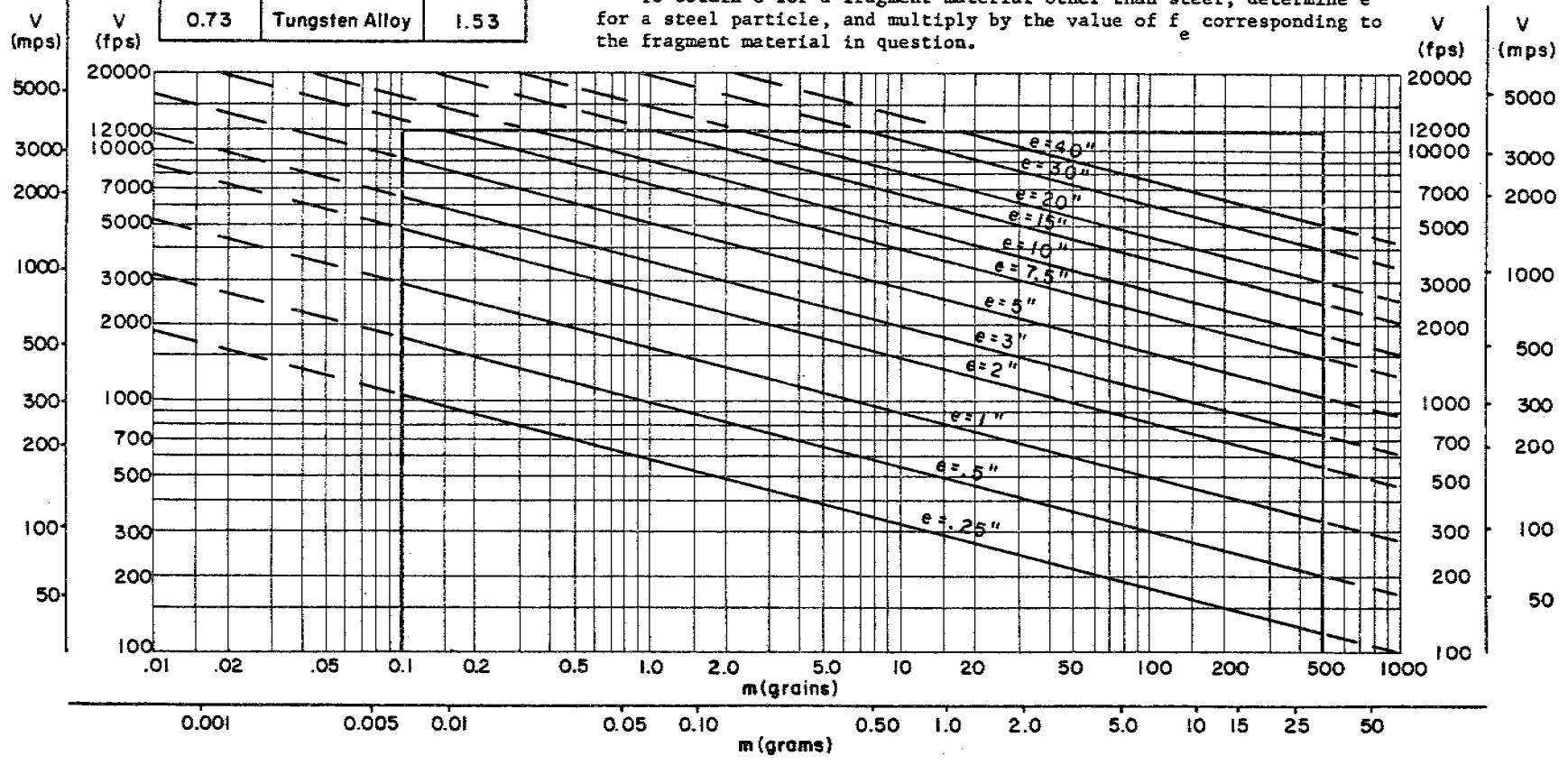


Fig. 9

## STEEL FRAGMENTS vs MAFTEX
## θ = 60°

| $f_v$ | Material | $f_e$ |
|---|---|---|
| 2.23 | Plastic | 0.34 |
| 2.09 | Mg Alloy | 0.37 |
| 1.60 | Al Alloy | 0.53 |
| 1.00 | Steel | 1.00 |
| 0.73 | Tungsten Alloy | 1.53 |

To obtain V for a fragment material other than steel, determine V for a steel particle, and multiply by the value of $f_v$ corresponding to the fragment material in question.

To obtain e for a fragment material other than steel, determine e for a steel particle, and multiply by the value of $f_e$ corresponding to the fragment material in question.

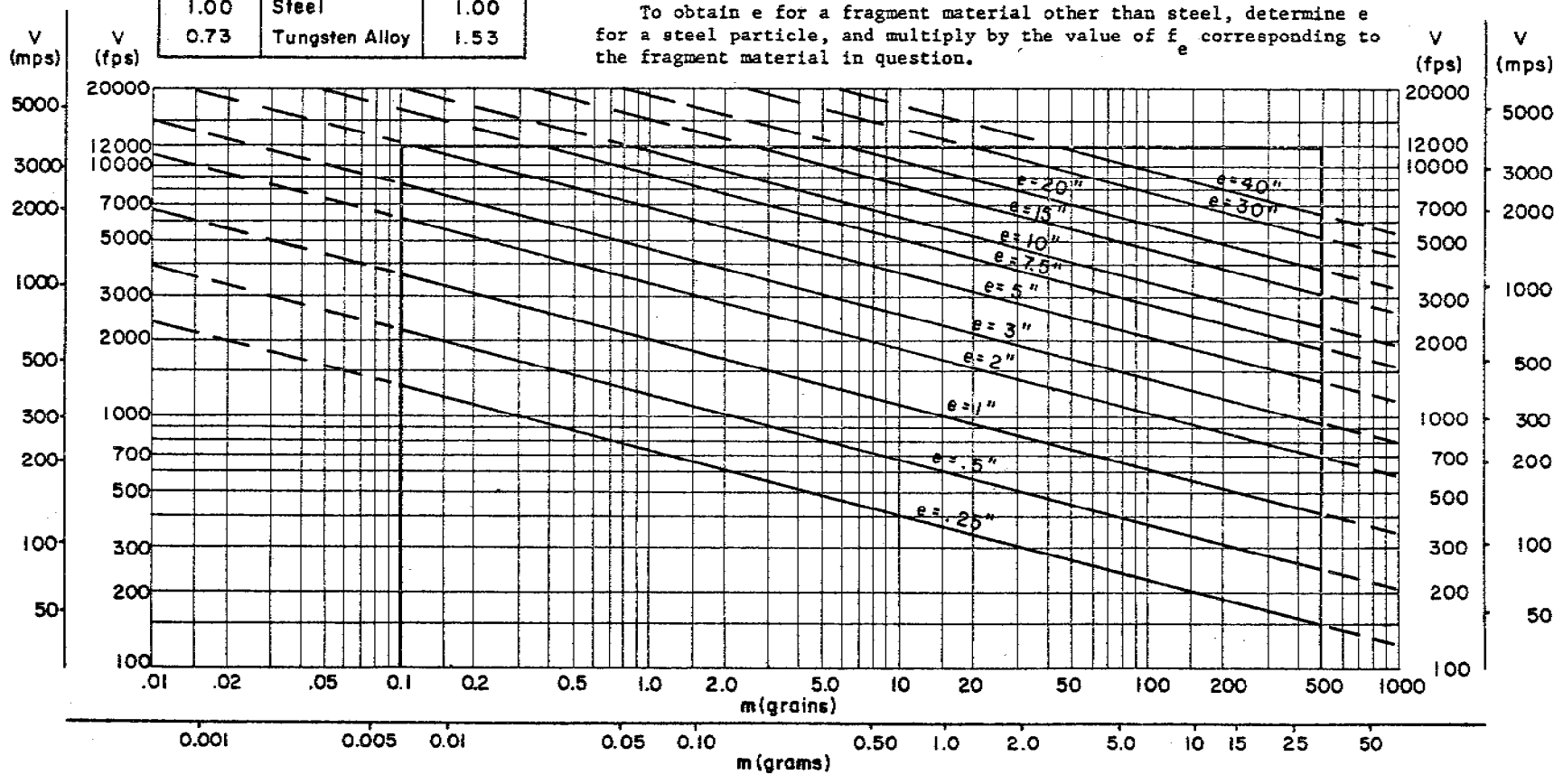


Fig. 10

| $f_v$ | Material | $f_e$ |
|---|---|---|
| 2.23 | Plastic | 0.34 |
| 2.09 | Mg Alloy | 0.37 |
| 1.60 | Al Alloy | 0.53 |
| 1.00 | Steel | 1.00 |
| 0.73 | Tungsten Alloy | 1.53 |

## STEEL FRAGMENTS vs MAFTEX
## $\theta = 70°$

To obtain V for a fragment material other than steel, determine V for a steel particle, and multiply by the value of $f_v$ corresponding to the fragment material in question.

To obtain e for a fragment material other than steel, determine e for a steel particle, and multiply by the value of $f_e$ corresponding to the fragment material in question.

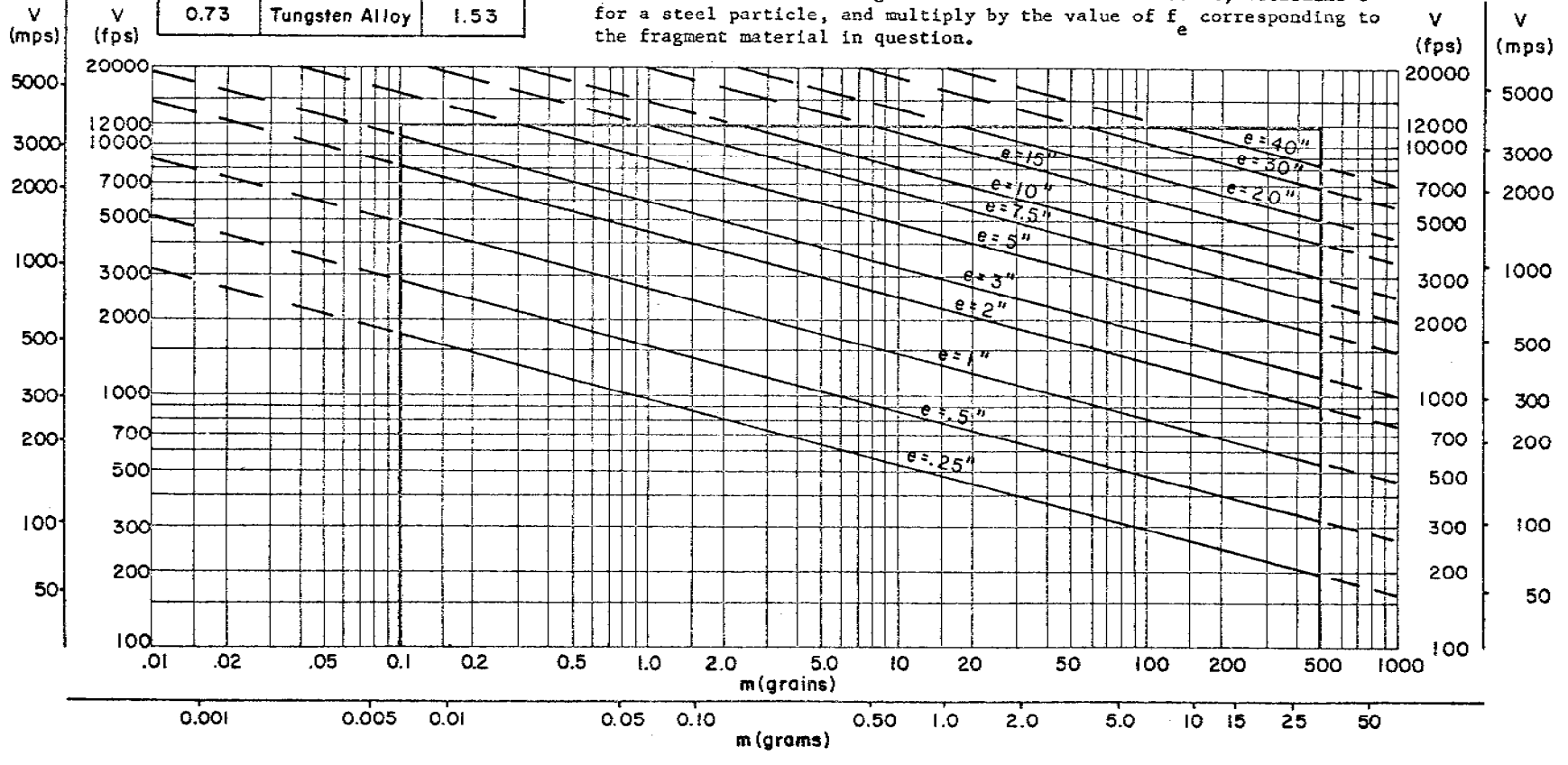


Fig. 11

## Depth of Penetration into Maftex Along Line of Travel vs $(mV^4)^{1/3}$

(Compact Fragments)

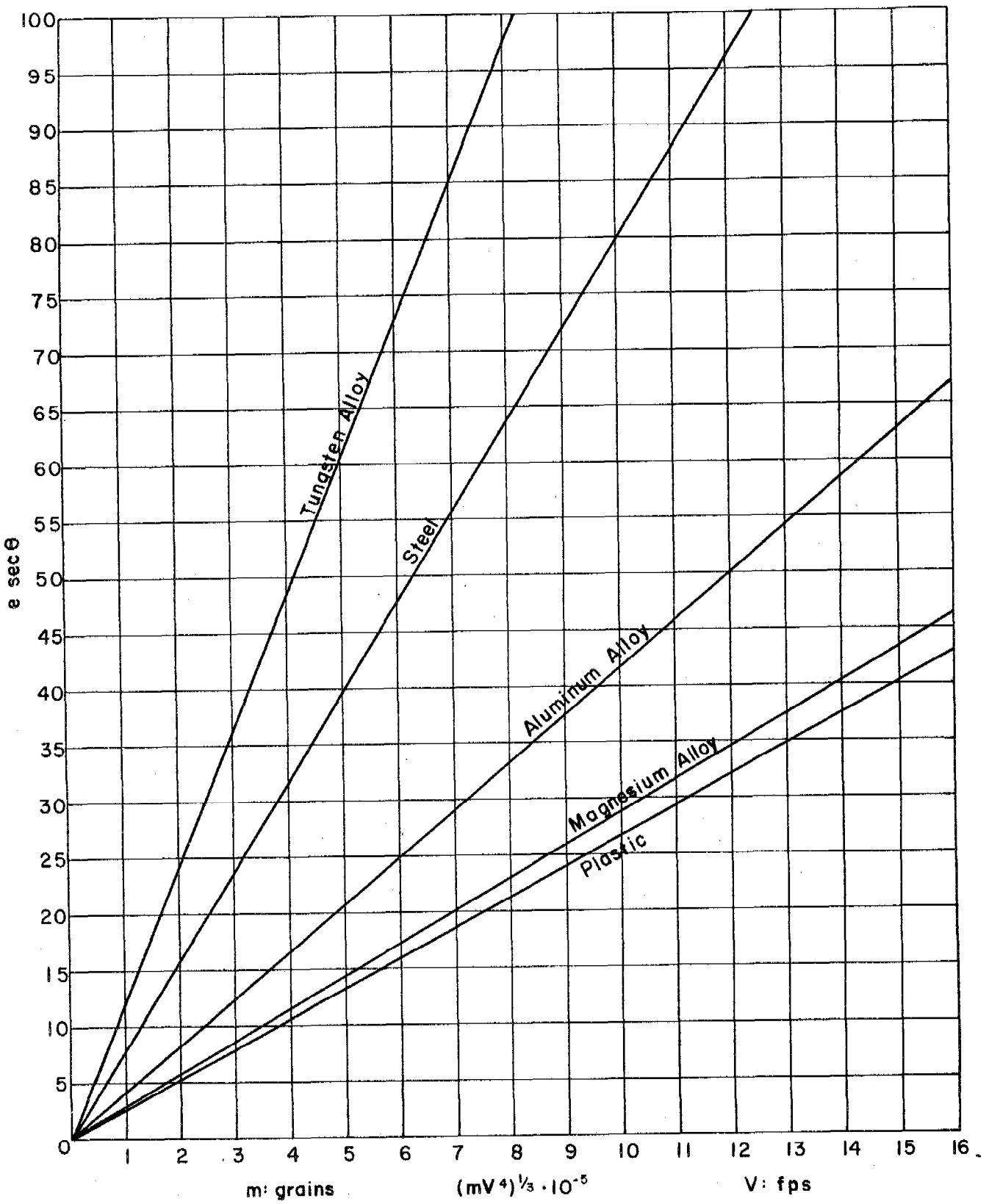


Fig. 12

## SUMMARY

A single formula covering several fragment materials has been established to determine particle velocity on the basis of the depth of penetration of the fragment into a variety of fiber board. This formula is:

$$V = 26170 \quad e^{0.736} \; m^{-0.681} \quad (\sec \theta)^{0.711} \quad A^{0.638}$$

where the symbols are defined in the section, EMPIRICAL RELATIONSHIPS. By replacing A with $cm^{2/3}$, where c depends on the fragment material, a set of equations is generated, one for each fragment material.

The velocity estimate for a material X can be obtained by multiplying the velocity estimate for steel by $f_V$, a constant for each material. The estimate of thickness of fiber board that will be penetrated by a fragment of material X can be obtained by multiplying the estimate of thickness of fiber board that will be penetrated by a steel fragment by $f_e$, a constant for each material.

The values for b and $\sigma$ (see Empirical Relationships) which describe the goodness of fit of the equation to the experimental data are given below.

For each fragment material a maximum velocity has been established under which the fragment is expected to remain essentially intact upon penetration of the particular medium, Maftex. The equation provided for the estimates of velocity for a given fragment material may not produce reasonable estimates beyond this maximum velocity. Whenever the fragment deforms or breaks up appreciably while penetrating the collecting medium, the fragment does not penetrate as far as would be expected.

Whereas the magnitude of $\sigma$ serves as an overall criterion for the goodness of fit of the formula to the entire body of data, the magnitude of the errors in the velocity estimates tends to increase with velocity.

The relative errors in the velocity estimates are highest at low velocity. One apparent reason for this is that the basic unit of thickness of Maftex for the experimental work was one sheet or one-half inch. A fragment found in the twentieth sheet of Maftex has penetrated between 9.5 and 10.0 inches of Maftex. No matter which figure is used, the relative error in this measurement will be small. However, a fragment found in the first (half-inch) sheet of Maftex has penetrated a thickness less than 0.5 inches of Maftex and the relative error in this measurement may be large. One technique which will permit better measurements of thickness penetrated is to use thinner pieces of Maftex for the first few sheets of the pack. In addition, an effort should be made to measure each depth of penetration to the nearest half or quarter sheet.

A series of graphs follows showing for each fragment material the variation with velocity of the percentage of error of the velocity estimates.

Table XII

Goodness of Fit of the Master Estimating Equation

| Fragment Material | Sample Size N | b (fps) | σ (fps) | Maximum Velocity for Estimates (fps) |
|---|---|---|---|---|
| Plastic | 19 | -36 | 678 | 4200 |
| Magnesium Alloy | 16 | -231 | 704 | 5500 |
| Aluminum Alloy | 42 | 11 | 819 | 8500 |
| Steel | 136 | 112 | 564 | 10000 |
| Tungsten Alloy | 36 | -70 | 814 | 8000 |
| All | 249 | 36 | 671 | ---- |

# VARIATION OF PERCENT ERROR IN VELOCITY ESTIMATES FOR 1000 FPS INTERVALS IN VELOCITY

Plastic Fragments

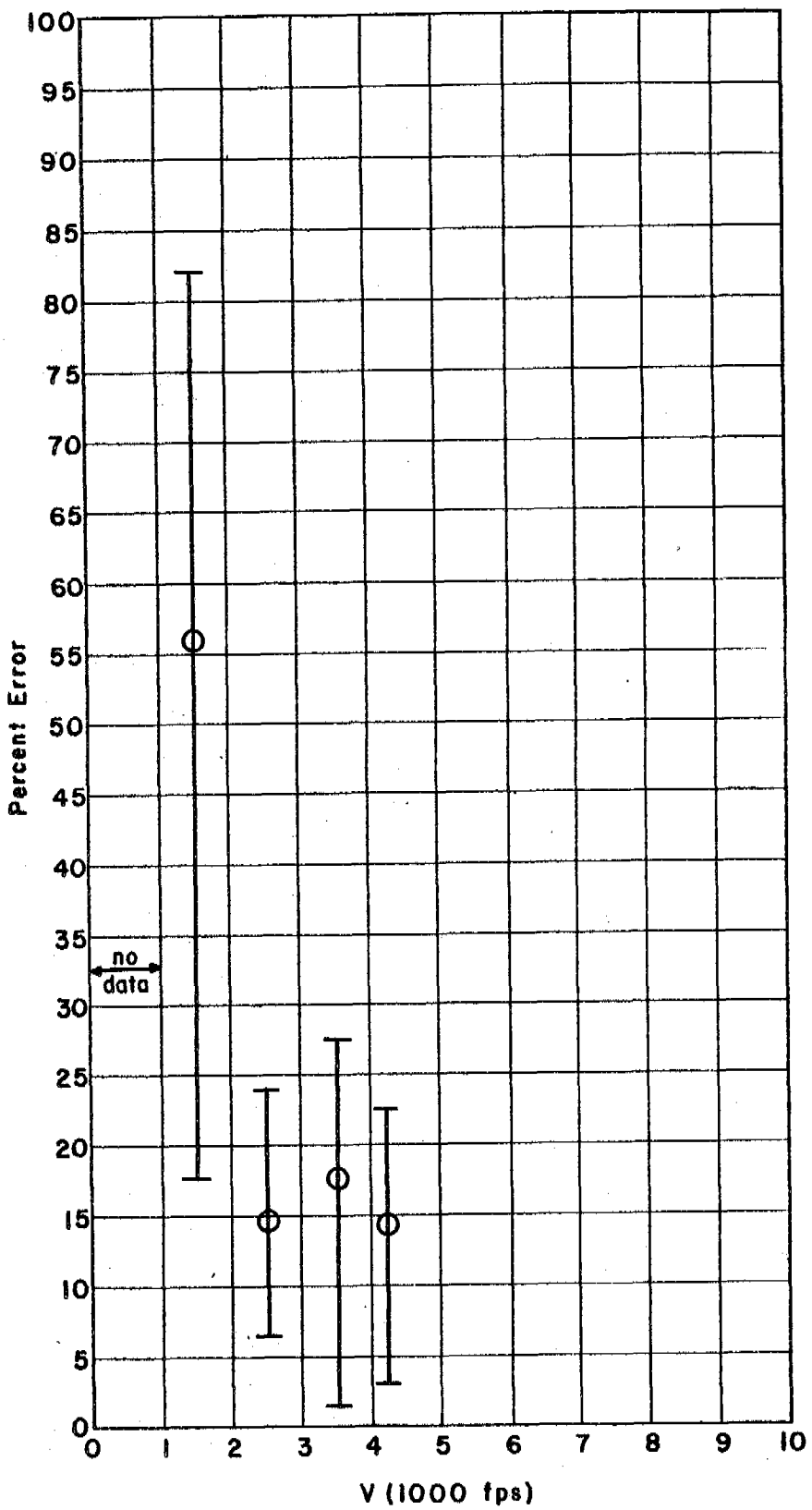


Notes:

1) ⊙ = average percent error in interval

2) $V_{max.}$ = 4200 fps

Fig. 13

# VARIATION OF PERCENT ERROR IN VELOCITY ESTIMATES FOR 1000 FPS INTERVALS IN VELOCITY

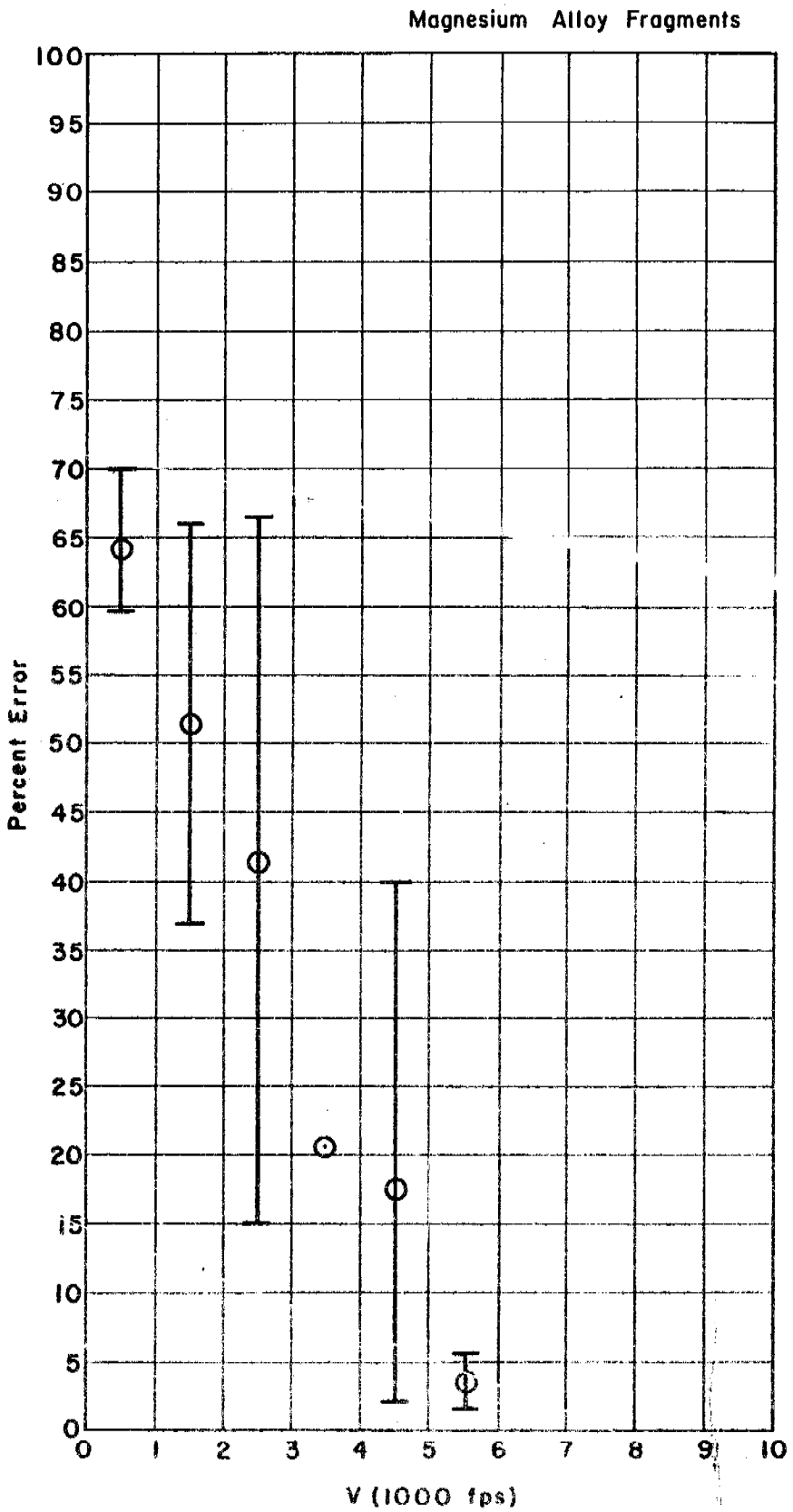


Notes:

1) ⊙ = average percent error in interval

2) $V_{max.}$ = 5500 fps

Fig. 14

# VARIATION OF PERCENT ERROR IN VELOCITY ESTIMATES FOR 1000 FPS INTERVALS IN VELOCITY

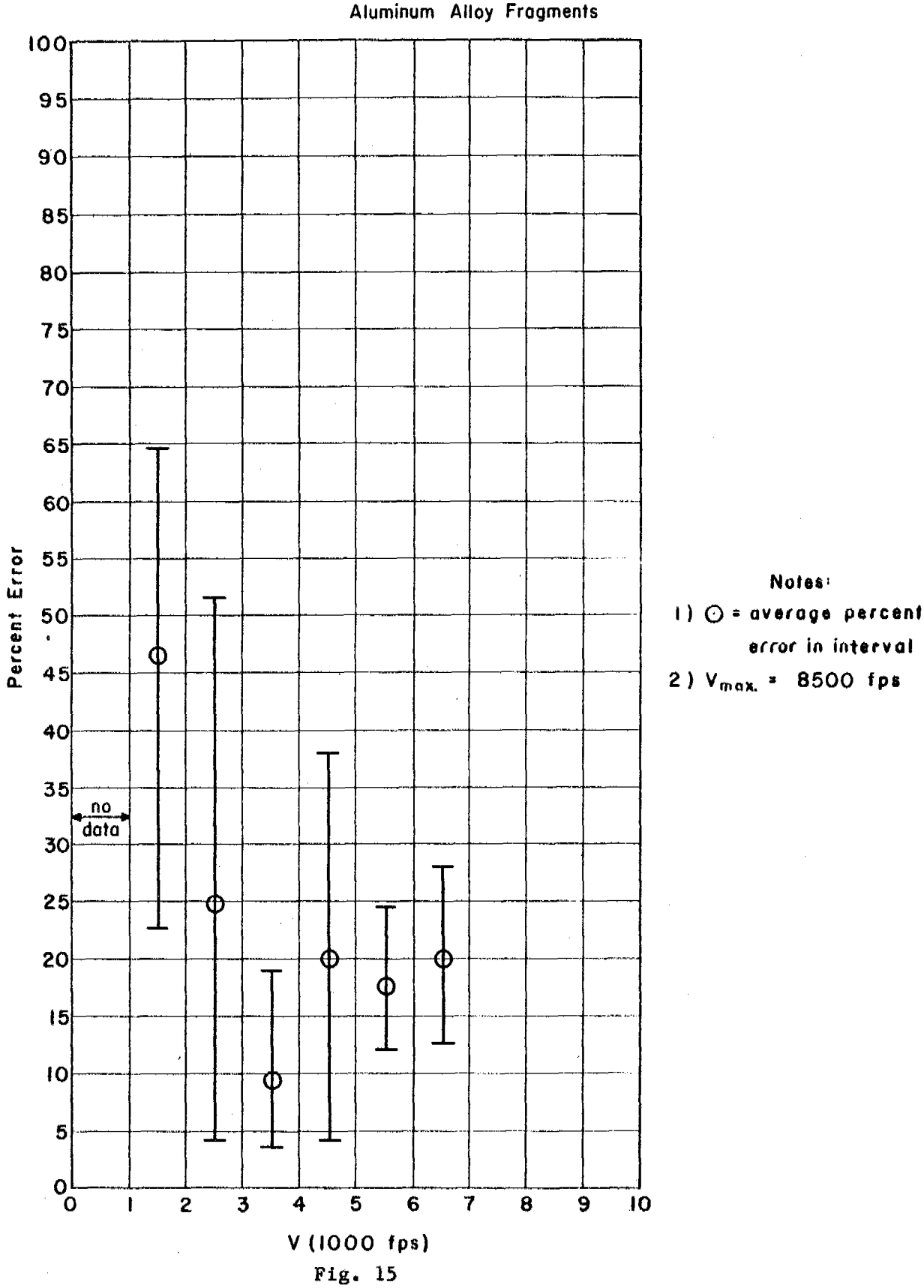


Fig. 15

# VARIATION OF PERCENT ERROR IN VELOCITY ESTIMATES FOR 1000 FPS INTERVALS IN VELOCITY

Steel Fragments

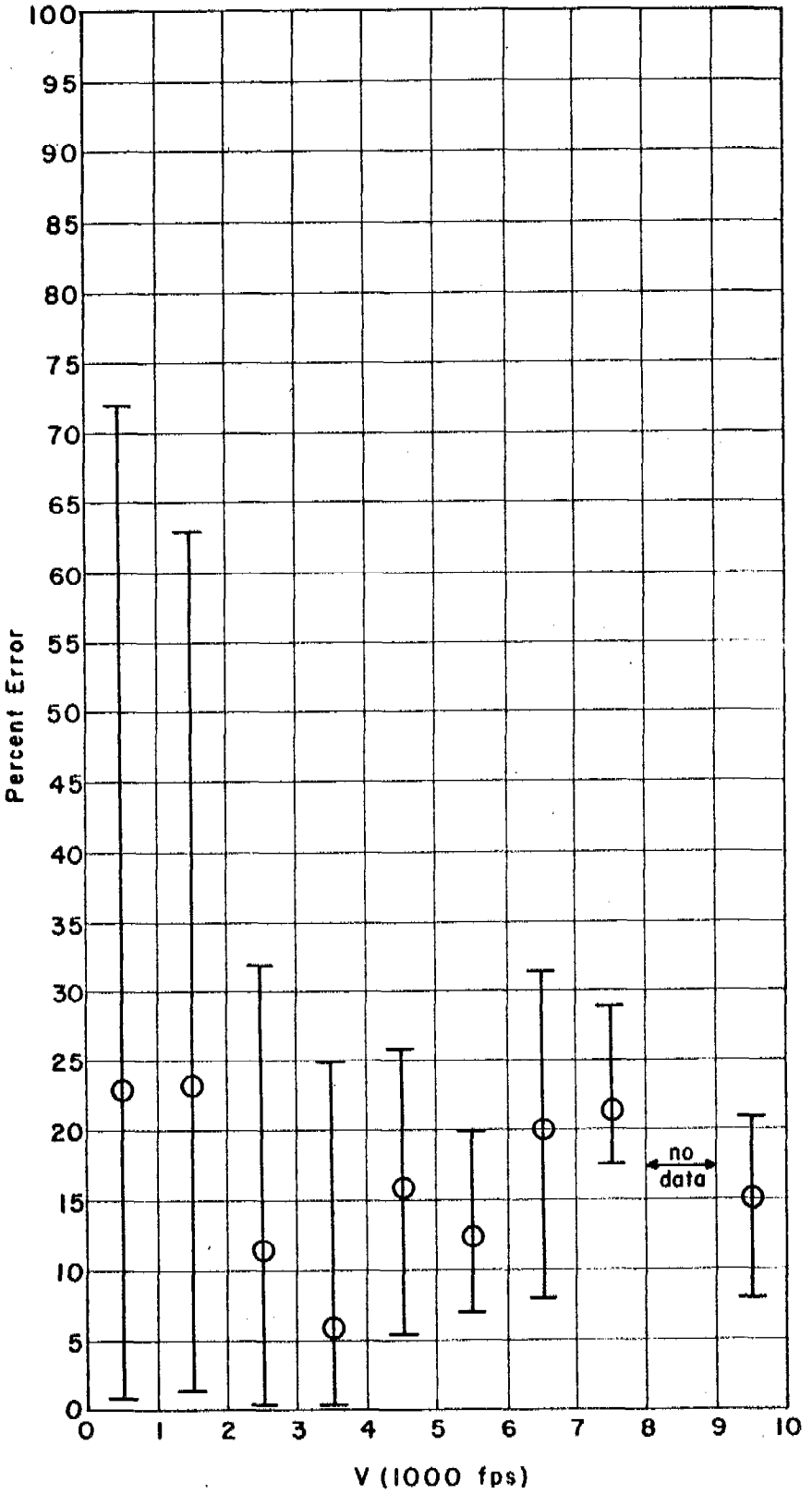


Notes:

1) ⊙ = average percent error in interval

2) $V_{max.}$ = 10,000 fps

Fig. 16

# VARIATION OF PERCENT ERROR IN VELOCITY ESTIMATES FOR 1000 FPS INTERVALS IN VELOCITY

Tungsten Alloy Fragments

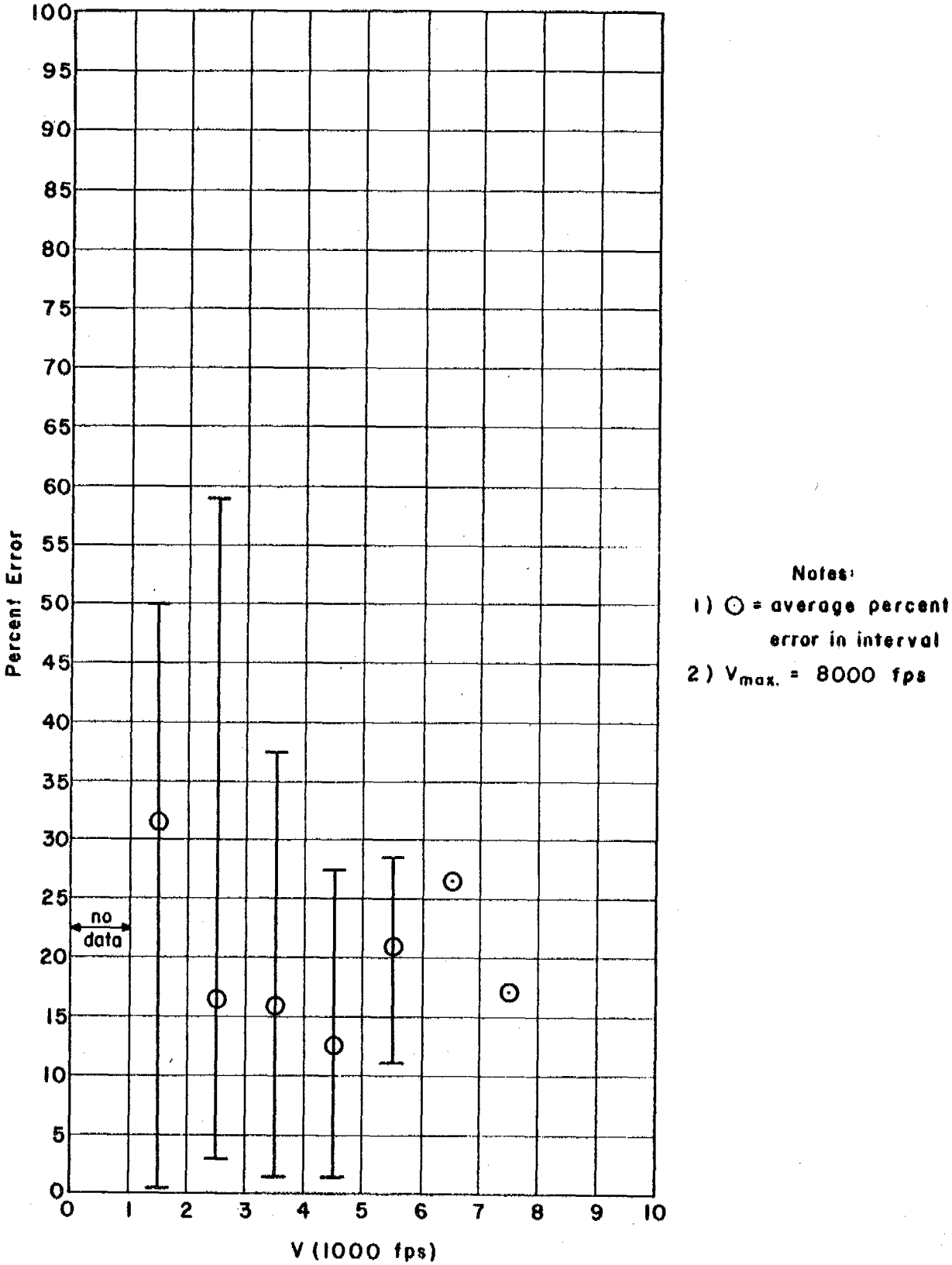


Fig. 17

# APPENDIX I

## CHARACTERISTICS OF EXPERIMENTAL DATA

TABLE XIII

Characteristics of Experimental Data

Plastic Fragments

| Data No. | m (grains) | $\theta$ (degrees) | V (fps) | e (inches) |
|---|---|---|---|---|
| 1 | 0.25 | 0 | 2600 | 0.75 |
| 2 | 0.25 | 70 | 2900 | 0.25 |
| 3* | 0.93 | 60 | 5314 | 0.25 |
| 4 | 0.99 | 0 | 4105 | 1.25 |
| 5 | 1.0 | 0 | 1950 | 0.75 |
| 6 | 1.0 | 0 | 3000 | 1.25 |
| 7 | 1.0 | 70 | 3500 | 0.7 |
| 8* | 1.0 | 0 | 4635 | 1.0 |
| 9 | 5.0 | 0 | 1350 | 1.5 |
| 10 | 5.0 | 0 | 3800 | 2.5 |
| 11 | 5.0 | 70 | 3400 | 1.0 |
| 12 | 15.0 | 0 | 1800 | 3.0 |
| 13 | 15.0 | 0 | 3750 | 3.0 |
| 14 | 15.0 | 70 | 2500 | 0.7 |
| 15 | 15.0 | 70 | 2500 | 1.0 |
| 16 | 15.0 | 70 | 3800 | 1.0 |
| 17* | 15.0 | 0 | 5800 | 2.5 |
| 18* | 15.35 | 0 | 5000 | 2.25 |
| 19* | 15.5 | 0 | 7150 | 3.0 |
| 20 | 30.0 | 0 | 4200 | 4.0 |
| 21* | 30.0 | 0 | 5460 | 4.0 |
| 22 | 30.0 | 70 | 1400 | 0.7 |
| 23* | 60.0 | 70 | 4500 | 1.5 |
| 24 | 120.0 | 0 | 4000 | 8.0 |
| 25* | 120.0 | 0 | 4545 | 7.0 |
| 26* | 120.0 | 0 | 5840 | 6.5 |
| 27* | 120.0 | 0 | 6600 | 6.5 |
| 28 | 120.0 | 70 | 3950 | 2.0 |
| 29* | 122.0 | 0 | 5525 | 6.5 |
| 30 | 124.0 | 0 | 1000 | 2.5 |

* Data point not included in analytical fit because of excessive fragment deformation or break-up.

TABLE XIV

Characteristics of Experimental Data

Magnesium Alloy Fragments

| Data No. | m (grains) | $\theta$ (degrees) | V (fps) | e (inches) |
|---|---|---|---|---|
| 1 | 0.1 | 0 | 2500 | 0.5 |
| 2 | 0.12 | 0 | 4180 | 0.7 |
| 3 | 0.25 | 0 | 3300 | 1.1 |
| 4 | 1.0 | 0 | 1600 | 0.75 |
| 5 | 1.0 | 0 | 4850 | 2.5 |
| 6* | 1.003 | 0 | 5925 | 2.25 |
| 7* | 1.005 | 60 | 5693 | 0.75 |
| 8 | 5.0 | 0 | 2000 | 2.5 |
| 9 | 5.0 | 0 | 4300 | 3.5 |
| 10 | 15.0 | 0 | 1400 | 2.0 |
| 11 | 15.0 | 0 | 4200 | 5.0 |
| 12 | 15.0 | 70 | 4100 | 1.1 |
| 13* | 15.35 | 0 | 7050 | 5.0 |
| 14 | 30.0 | 0 | 970 | 1.6 |
| 15* | 30.0 | 0 | 6780 | 7.0 |
| 16* | 60.0 | 0 | 6450 | 9.0 |
| 17* | 60.0 | 0 | 7000 | 5.5 |
| 18 | 60.0 | 70 | 4400 | 2.0 |
| 19 | 120.0 | 0 | 850 | 2.1 |
| 20 | 120.0 | 0 | 5460 | 13.0 |
| 21 | 120.0 | 70 | 2030 | 2.1 |
| 22 | 120.0 | 70 | 5000 | 4.5 |

* Data point not included in analytical fit because of excessive fragment deformation or break-up.

TABLE XV

Characteristics of Experimental Data

Aluminum Alloy Fragments

| Data No. | m (grains) | $\theta$ (degrees) | V (fps) | e (inches) |
|---|---|---|---|---|
| 1 | 0.1 | 0 | 2975 | 0.75 |
| 2 | 0.1 | 60 | 2908 | 0.437 |
| 3 | 0.1 | 70 | 3223 | 0.25 |
| 4 | 0.108 | 0 | 2299 | 0.75 |
| 5 | 0.115 | 0 | 4842 | 1.0 |
| 6 | 0.24 | 60 | 2807 | 0.5 |
| 7 | 0.258 | 0 | 1153 | 0.5 |
| 8 | 0.258 | 70 | 3277 | 0.5 |
| 9 | 0.951 | 60 | 1798 | 0.75 |
| 10 | 0.951 | 70 | 2521 | 0.375 |
| 11 | 0.972 | 0 | 6420 | 3.5 |
| 12 | 1.0 | 0 | 5016 | 4.0 |
| 13 | 1.0 | 0 | 6430 | 4.0 |
| 14 | 1.03 | 0 | 1462 | 0.875 |
| 15 | 1.03 | 60 | 1934 | 0.75 |
| 16 | 1.03 | 70 | 2191 | 0.375 |
| 17 | 5.0 | 0 | 1612 | 2.5 |
| 18 | 5.0 | 0 | 2000 | 3.0 |
| 19 | 5.0 | 70 | 2516 | 1.0 |
| 20 | 5.25 | 60 | 1470 | 1.0 |
| 21 | 5.25 | 60 | 2244 | 1.5 |
| 22 | 5.45 | 60 | 2465 | 1.5 |
| 23 | 5.5 | 70 | 4010 | 1.5 |
| 24 | 5.5 | 70 | 4634 | 1.0 |
| 25 | 15.0 | 0 | 1734 | 3.5 |
| 26 | 15.0 | 0 | 2362 | 5.5 |
| 27 | 15.0 | 0 | 5323 | 6.5 |
| 28 | 15.0 | 0 | 6204 | 7.5 |
| 29 | 15.5 | 0 | 2090 | 4.5 |
| 30* | 15.5 | 0 | 9375 | 5.75 |

* Data point not included in analytical fit because of excessive fragment deformation or break-up.

TABLE XV (CONT)

Characteristics of Experimental Data

Aluminum Alloy Fragments

| Data No. | m (grains) | $\theta$ (degrees) | V (fps) | e (inches) |
|---|---|---|---|---|
| 31 | 15.6 | 0 | 4485 | 5.75 |
| 32* | 15.6 | 0 | 11200 | ---- |
| 33 | 30.0 | 0 | 3600 | 8.5 |
| 34 | 31.0 | 0 | 5290 | 9.0 |
| 35 | 31.0 | 60 | 3391 | 3.0 |
| 36 | 31.0 | 70 | 4299 | 2.0 |
| 37 | 62.0 | 0 | 3912 | 10.0 |
| 38 | 62.0 | 60 | 3929 | 5.0 |
| 39 | 63.0 | 70 | 5520 | 5.0 |
| 40 | 120.0 | 0 | 7182 | 15.0 |
| 41 | 122.0 | 0 | 3933 | 14.0 |
| 42 | 122.0 | 60 | 4454 | 8.5 |
| 43 | 232.0 | 0 | 3948 | 18.5 |
| 44 | 240.0 | 0 | 6092 | 21.5 |
| 45 | 243.0 | 70 | 3777 | 7.0 |
| 46 | 244.0 | 60 | 3219 | 7.5 |

* Data point not included in analytical fit because of excessive deformation or break-up.

TABLE XVI

Characteristics of Experimental Data

Steel Fragments

| Data No. | m (grains) | $\theta$ (degrees) | V (fps) | e (inches) |
|---|---|---|---|---|
| 1 | 0.057 | 60 | 3700 | 0.75 |
| 2 | 0.059 | 0 | 2600 | 1.375 |
| 3 | 0.059 | 70 | 4150 | 0.625 |
| 4 | 0.112 | 0 | 6560 | 3.5 |
| 5 | 0.225 | 0 | 9103 | 7.0 |
| 6 | 0.225 | 0 | 9337 | 8.0 |
| 7* | 0.225 | 0 | 11109 | 8.0 |
| 8 | 0.236 | 0 | 1015 | 1.0 |
| 9 | 0.236 | 0 | 2750 | 2.75 |
| 10 | 0.236 | 60 | 2100 | 1.563 |
| 11 | 0.236 | 70 | 3440 | 1.25 |
| 12 | 0.825 | 0 | 6767 | 9.0 |
| 13 | 0.825 | 0 | 7613 | 9.5 |
| 14* | 0.825 | 0 | 12799 | 11.5 |
| 15 | 0.826 | 0 | 1210 | 1.25 |
| 16 | 0.826 | 0 | 2500 | 3.88 |
| 17 | 0.826 | 60 | 1540 | 1.125 |
| 18 | 0.826 | 60 | 1840 | 1.44 |
| 19 | 0.826 | 70 | 3000 | 1.568 |
| 20 | 0.826 | 70 | 3270 | 1.75 |
| 21* | 0.84 | 0 | 12480 | 10.5 |
| 22 | 0.952 | 0 | 7050 | 7.0 |
| 23* | 1.98 | 0 | 11100 | 15.5 |
| 24 | 2.5 | 0 | 900 | 0.39 |
| 25 | 2.5 | 0 | 1000 | 0.5 |
| 26 | 2.5 | 0 | 1400 | 1.11 |
| 27 | 5.0 | 0 | 600 | 0.59 |
| 28 | 5.0 | 0 | 800 | 0.67 |
| 29 | 5.0 | 0 | 1000 | 1.04 |
| 30 | 5.0 | 0 | 1100 | 1.35 |

* Data point not included in analytical fit because of excessive deformation or break-up.

TABLE XVI (CONT)

Characteristics of Experimental Data

Steel Fragments

| Data No. | m (grains) | $\theta$ (degrees) | V (fps) | e (inches) |
|---|---|---|---|---|
| 31 | 5.0 | 0 | 1200 | 1.8 |
| 32 | 5.0 | 0 | 1300 | 1.94 |
| 33 | 5.0 | 0 | 1400 | 1.94 |
| 34 | 5.0 | 0 | 1500 | 2.35 |
| 35* | 6.75 | 0 | 15500 | 21.5 |
| 36 | 10.0 | 0 | 400 | 0.25 |
| 37 | 10.0 | 0 | 500 | 0.61 |
| 38 | 10.0 | 0 | 600 | 0.75 |
| 39 | 10.0 | 0 | 800 | 1.52 |
| 40 | 10.0 | 0 | 900 | 1.13 |
| 41 | 10.0 | 0 | 1000 | 2.16 |
| 42 | 10.0 | 0 | 1100 | 1.0 |
| 43 | 10.0 | 0 | 1200 | 2.08 |
| 44 | 15.0 | 0 | 400 | 1.08 |
| 45 | 15.0 | 0 | 500 | 0.25 |
| 46 | 15.0 | 0 | 600 | 1.25 |
| 47 | 15.0 | 0 | 700 | 1.25 |
| 48 | 15.0 | 0 | 800 | 1.92 |
| 49 | 15.0 | 0 | 900 | 1.88 |
| 50 | 15.0 | 0 | 1000 | 2.32 |
| 51 | 15.0 | 0 | 1100 | 2.31 |
| 52 | 15.0 | 0 | 1200 | 3.0 |
| 53 | 15.0 | 0 | 1300 | 2.75 |
| 54 | 15.0 | 0 | 1400 | 3.58 |
| 55 | 15.0 | 0 | 1500 | 3.25 |
| 56 | 15.0 | 0 | 1685 | 5.17 |
| 57 | 15.0 | 0 | 1960 | 5.17 |
| 58 | 15.0 | 0 | 2010 | 4.95 |
| 59 | 15.0 | 0 | 2075 | 5.0 |
| 60 | 15.0 | 0 | 2400 | 5.17 |

* Data point not included in analytical fit because of excessive fragment deformation or break-up.

TABLE XVI (CONT)

Characteristics of Experimental Data

Steel Fragments

| Data No. | m (grains) | $\theta$ (degrees) | V (fps) | e (inches) |
|---|---|---|---|---|
| 61 | 15.0 | 0 | 7925 | 18.75 |
| 62 | 15.0 | 0 | 9920 | 18.0 |
| 63* | 29.2 | 0 | 10682 | 26.0 |
| 64 | 30.0 | 0 | 758 | 2.2 |
| 65 | 30.0 | 0 | 854 | 2.25 |
| 66 | 30.0 | 0 | 886 | 2.25 |
| 67 | 30.0 | 0 | 890 | 2.25 |
| 68 | 30.0 | 0 | 907 | 2.25 |
| 69 | 30.0 | 0 | 951 | 2.3 |
| 70 | 30.0 | 0 | 3413 | 10.4 |
| 71 | 30.0 | 0 | 3448 | 11.9 |
| 72 | 30.0 | 0 | 3484 | 10.3 |
| 73 | 30.0 | 0 | 4651 | 15.0 |
| 74 | 30.0 | 0 | 4739 | 15.0 |
| 75 | 30.0 | 0 | 4854 | 15.5 |
| 76 | 30.0 | 45 | 3939 | 11.5 |
| 77 | 30.0 | 45 | 5887 | 15.5 |
| 78 | 30.0 | 45 | 5887 | 15.5 |
| 79 | 30.0 | 60 | 3170 | 6.0 |
| 80 | 30.0 | 60 | 5957 | 10.0 |
| 81 | 30.0 | 70 | 4935 | 6.0 |
| 82 | 60.0 | 0 | 632 | 2.0 |
| 83 | 60.0 | 0 | 693 | 2.0 |
| 84 | 60.0 | 0 | 875 | 2.5 |
| 85 | 60.0 | 0 | 1155 | 5.0 |
| 86 | 60.0 | 0 | 1157 | 6.0 |
| 87 | 60.0 | 0 | 1460 | 6.0 |
| 88 | 60.0 | 0 | 1466 | 5.0 |
| 89 | 60.0 | 0 | 1848 | 7.5 |
| 90 | 60.0 | 0 | 1887 | 8.0 |

* Data point not included in analytical fit because of excessive fragment deformation or break-up.

TABLE XVI (CONT)

Characteristics of Experimental Data

Steel Fragments

| Data No. | m (grains) | $\theta$ (degrees) | V (fps) | e (inches) |
|---|---|---|---|---|
| 91 | 60.0 | 0 | 2130 | 8.0 |
| 92 | 60.0 | 0 | 2268 | 10.0 |
| 93 | 60.0 | 0 | 2315 | 10.0 |
| 94 | 60.0 | 0 | 2463 | 8.5 |
| 95 | 60.0 | 0 | 2725 | 10.0 |
| 96 | 60.0 | 0 | 2762 | 12.0 |
| 97 | 60.0 | 0 | 3125 | 13.5 |
| 98 | 60.0 | 0 | 3135 | 14.5 |
| 99 | 60.0 | 0 | 3584 | 15.0 |
| 100 | 60.0 | 0 | 3690 | 15.0 |
| 101 | 60.0 | 0 | 3788 | 15.0 |
| 102 | 60.0 | 0 | 4651 | 16.5 |
| 103 | 60.0 | 0 | 4673 | 15.5 |
| 104 | 60.0 | 0 | 4762 | 18.5 |
| 105 | 60.0 | 0 | 10600 | 24.5 |
| 106 | 60.0 | 45 | 2485 | 8.5 |
| 107 | 60.0 | 45 | 5191 | 16.0 |
| 108 | 60.0 | 60 | 3848 | 9.5 |
| 109 | 60.0 | 70 | 4098 | 5.5 |
| 110 | 120.0 | 45 | 2718 | 12.0 |
| 111 | 120.0 | 45 | 3147 | 13.0 |
| 112 | 120.0 | 45 | 3165 | 13.5 |
| 113 | 120.0 | 45 | 3203 | 14.0 |
| 114 | 120.0 | 45 | 3212 | 14.0 |
| 115 | 120.0 | 60 | 3040 | 10.0 |
| 116 | 120.0 | 70 | 5118 | 9.5 |
| 117 | 240.0 | 0 | 341 | 1.2 |
| 118 | 240.0 | 0 | 400 | 0.4 |
| 119 | 240.0 | 0 | 449 | 0.4 |
| 120 | 240.0 | 0 | 531 | 2.5 |

TABLE XVI (CONT)

Characteristics of Experimental Data

Steel Fragments

| Data No. | m (grains) | $\theta$ (degrees) | V (fps) | e (inches) |
|---|---|---|---|---|
| 121 | 240.0 | 0 | 809 | 4.3 |
| 122 | 240.0 | 0 | 988 | 7.0 |
| 123 | 240.0 | 0 | 1205 | 10.3 |
| 124 | 240.0 | 0 | 1299 | 12.0 |
| 125 | 240.0 | 0 | 1422 | 10.8 |
| 126 | 240.0 | 0 | 1502 | 11.0 |
| 127 | 240.0 | 0 | 1669 | 14.0 |
| 128 | 240.0 | 0 | 1745 | 12.2 |
| 129 | 240.0 | 0 | 2203 | 12.8 |
| 130 | 240.0 | 0 | 2882 | 20.5 |
| 131 | 240.0 | 0 | 3021 | 22.8 |
| 132 | 240.0 | 0 | 3115 | 24.5 |
| 133 | 240.0 | 0 | 3236 | 26.0 |
| 134 | 240.0 | 0 | 4115 | 24.0 |
| 135 | 240.0 | 0 | 4739 | 44.5 |
| 136 | 240.0 | 0 | 4831 | 34.3 |
| 137 | 240.0 | 0 | 4854 | 42.5 |
| 138 | 240.0 | 0 | 4878 | 36.5 |
| 139 | 240.0 | 0 | 5076 | 36.7 |
| 140 | 240.0 | 0 | 5076 | 38.8 |
| 141 | 240.0 | 0 | 6080 | 33.0 |
| 142 | 240.0 | 45 | 2271 | 15.0 |
| 143 | 240.0 | 45 | 2908 | 19.0 |
| 144 | 240.0 | 60 | 3129 | 13.0 |
| 145 | 240.0 | 60 | 3922 | 16.5 |
| 146 | 240.0 | 60 | 3922 | 16.5 |
| 147 | 240.0 | 70 | 5143 | 14.0 |
| 148 | 481.0 | 0 | 5225 | 52.5 |

TABLE XVII

Characteristics of Experimental Data

Tungsten Alloy Fragments

| Data No. | m (grains) | $\theta$ (degrees) | V (fps) | e (inches) |
|---|---|---|---|---|
| 1 | 0.112 | 0 | 3766 | 3.875 |
| 2 | 0.112 | 0 | 4871 | 4.125 |
| 3 | 0.114 | 0 | 6750 | 5.0 |
| 4 | 0.119 | 60 | 3782 | 1.75 |
| 5 | 0.119 | 70 | 4722 | 1.062 |
| 6 | 0.12 | 70 | 3446 | 1.125 |
| 7* | 0.128 | 0 | 9575 | 3.75 |
| 8 | 0.25 | 0 | 2262 | 2.5 |
| 9 | 0.256 | 0 | 1142 | 0.875 |
| 10 | 0.256 | 60 | 2398 | 1.25 |
| 11 | 0.256 | 70 | 3741 | 1.25 |
| 12 | 0.982 | 60 | 7200 | 6.0 |
| 13* | 1.0 | 0 | 9750 | 9.25 |
| 14* | 1.008 | 0 | 10075 | 8.75 |
| 15 | 1.05 | 0 | 1962 | 3.875 |
| 16 | 1.05 | 0 | 2143 | 4.375 |
| 17 | 1.05 | 60 | 2263 | 2.0 |
| 18 | 1.05 | 70 | 3041 | 2.25 |
| 19* | 1.1 | 0 | 16800 | 10.5 |
| 20 | 4.7 | 0 | 2393 | 5.5 |
| 21 | 4.95 | 70 | 5631 | 4.5 |
| 22 | 5.0 | 0 | 1478 | 5.5 |
| 23 | 5.0 | 0 | 5756 | 14.5 |
| 24* | 5.0 | 0 | 16150 | 21.0 |
| 25 | 5.0 | 60 | 2073 | 5.0 |
| 26 | 5.0 | 60 | 3844 | 9.5 |
| 27 | 5.25 | 70 | 5298 | 8.0 |
| 28 | 12.8 | 0 | 1701 | 10.0 |
| 29 | 12.8 | 0 | 4457 | 22.5 |
| 30* | 13.0 | 0 | 9070 | 28.25 |

* Data point not included in analytical fit because of excessive fragment deformation or break-up.

TABLE XVII (CONT)

Characteristics of Experimental Data

Tungsten Alloy Fragments

| Data No. | m (grains) | $\theta$ (degrees) | V (fps) | e (inches) |
|---|---|---|---|---|
| 31* | 13.0 | 0 | 10225 | 26.25 |
| 32* | 15.0 | 0 | 8260 | 31.0 |
| 33 | 29.2 | 0 | 3408 | 28.0 |
| 34* | 29.2 | 0 | 9300 | 35.25 |
| 35 | 29.2 | 60 | 3574 | 13.0 |
| 36 | 29.25 | 0 | 2604 | 16.0 |
| 37* | 29.3 | 0 | 9140 | 27.5 |
| 38 | 29.6 | 0 | 2995 | 18.0 |
| 39 | 31.0 | 70 | 3883 | 12.5 |
| 40 | 59.0 | 0 | 3603 | 35.0 |
| 41 | 59.0 | 70 | 5667 | 12.0 |
| 42* | 59.3 | 0 | 9480 | 36.0 |
| 43 | 59.45 | 60 | 3779 | 13.0 |
| 44 | 59.6 | 0 | 3949 | 33.0 |
| 45* | 60.1 | 0 | 9450 | 58.25 |
| 46 | 136.0 | 0 | 4103 | 54.0 |
| 47 | 136.0 | 60 | 4183 | 19.5 |
| 48 | 137.0 | 60 | 4306 | 23.0 |
| 49 | 238.0 | 60 | 2953 | 19.0 |
| 50 | 238.0 | 70 | 4400 | 16.5 |

* Data point not included in analytical fit because of excessive fragment deformation or break-up.

# APPENDIX II

## FRAGMENT RETARDATION IN AIR

## FRAGMENT RETARDATION IN AIR

The fragment velocities recorded in the experimental work were measured at a short distance before the collecting medium. The effect of drag even for short distances is significant for small particles. Hence it was necessary to correct the instrumental velocities for the effect of drag in order to obtain the fragment velocity at impact on the collecting medium. Corrections were based on the substance of BRLM Report 915 entitled, "Air Drag Measurements of Fragments" (U). For the reader's convenience, a brief summary of this report is given below along with a set of graphs indicating how fragment slow-down varies with velocity and fragment size for each fragment material.

The experimental work for BRLM 915 amounted to firing individual fragments with velocities from 600 to 5000 fps through three successive wire velocity grids. The average velocity over measured distances was obtained; the loss in velocity for a known distance of travel led to an estimate of the drag coefficient, $C_D$, for the fragment shape under consideration. Cubes, right circular cylinders, parallelepipeds, and shell fragments were used in the experimental work. All the fragments were steel,— ranging in weight from about 0.7 grains to 555 grains.

The retardation equation is taken to be:

$$\frac{dV}{dR} = - C_D \frac{A^*}{m} \rho V.$$

In this equation

V is the fragment velocity in fps,

R is the distance of travel in inches,

$C_D$ is the drag coefficient ($\sim$0.56 for cubical fragments with Mach numbers from 1 to 5 at sea level),

A* is the average projected area, in square inches, of the moving fragment in a plane perpendicular to its trajectory,

m is the fragment weight, in grains, and

$\rho$ is the air density in grains/(inch)$^3$; $\rho = 0.327$ at sea level (standard conditions)

If the fragments are randomly oriented in flight, then A* = A where

$$A = cm^{2/3}$$

and c is a constant for any homologous class of regularly shaped fragments. A value of c for the set of fragments for each fragment material has been given earlier in this report, but will be shown again in a table which follows shortly.

Therefore,

$$\frac{dV}{dR} = - \frac{C_D \, c \, \rho \, V}{m^{1/3}} .$$

Thus, with the initial value $V = V_o$ at $R = 0$, the differential equation has the solution

$$V = V_o \exp \left(-C_D \, c \, \rho \, R/m^{1/3}\right).$$

Let R be 12 inches, and let $\Delta V$ be the loss in velocity sustained by the fragment in this one foot of travel at sea level (standard conditions); then

$$\Delta V = V_o - V = V_o \left[ 1 - \exp \left(-h/m^{1/3}\right) \right]$$

where

$$h = C_D \, c \, (.327) \, (12).$$

Appropriate values for c and h for each of the fragment materials under consideration are given in the following table.

| Fragment Material | c | h |
|---|---|---|
| Plastic | 0.0308 | 0.0677 |
| Magnesium Alloy | 0.0279 | 0.0613 |
| Aluminum Alloy | 0.0103 | 0.0402 |
| Steel | 0.0088 | 0.0193 |
| Tungsten Alloy | 0.0054 | 0.0119 |

A set of graphs follows, showing for each fragment material the estimated loss in fragment velocity for one foot of travel. The assumptions that are implicit for the construction of these graphs are:

1) the value of $C_D$ is approximately 0.56 for all velocities, fragment weights, and fragment shapes under consideration,

2) the fragments are moving at, or near, sea-level (standard conditions),

3) the fragments move through air with no apparent stabilization regardless of the size, material, velocity, etc.

## Retardation for Plastic Fragments in Air

Notes:
a) Fragment has moved only one foot
b) Fragment moving at standard, sea-level conditions
c) $C_D \sim 0.56$

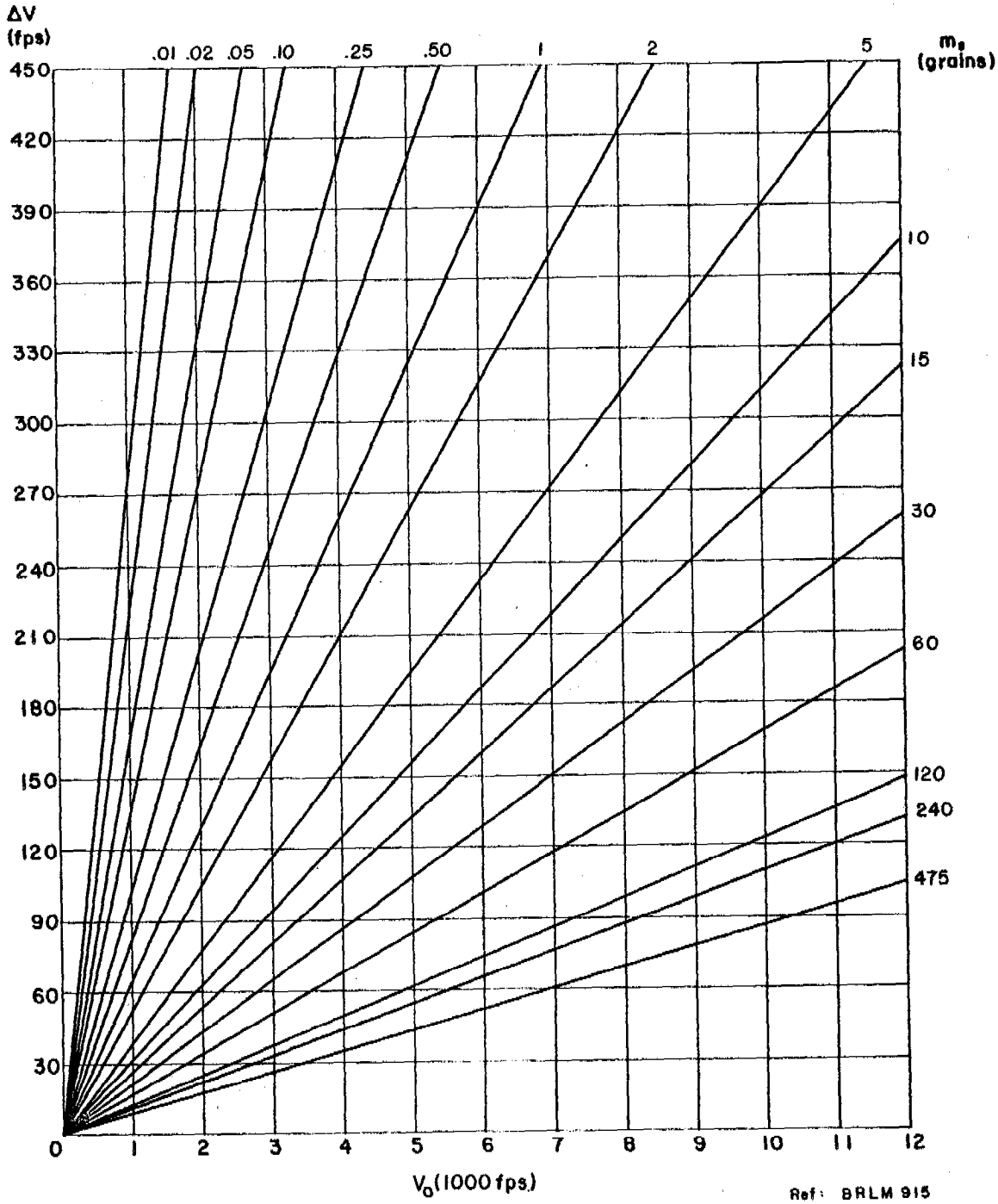


Fig. 18

## Retardation for Magnesium Alloy Fragments in Air

Notes:
a) Fragment has moved only one foot
b) Fragment moving at standard, sea-level conditions
c) $C_D \sim 0.56$

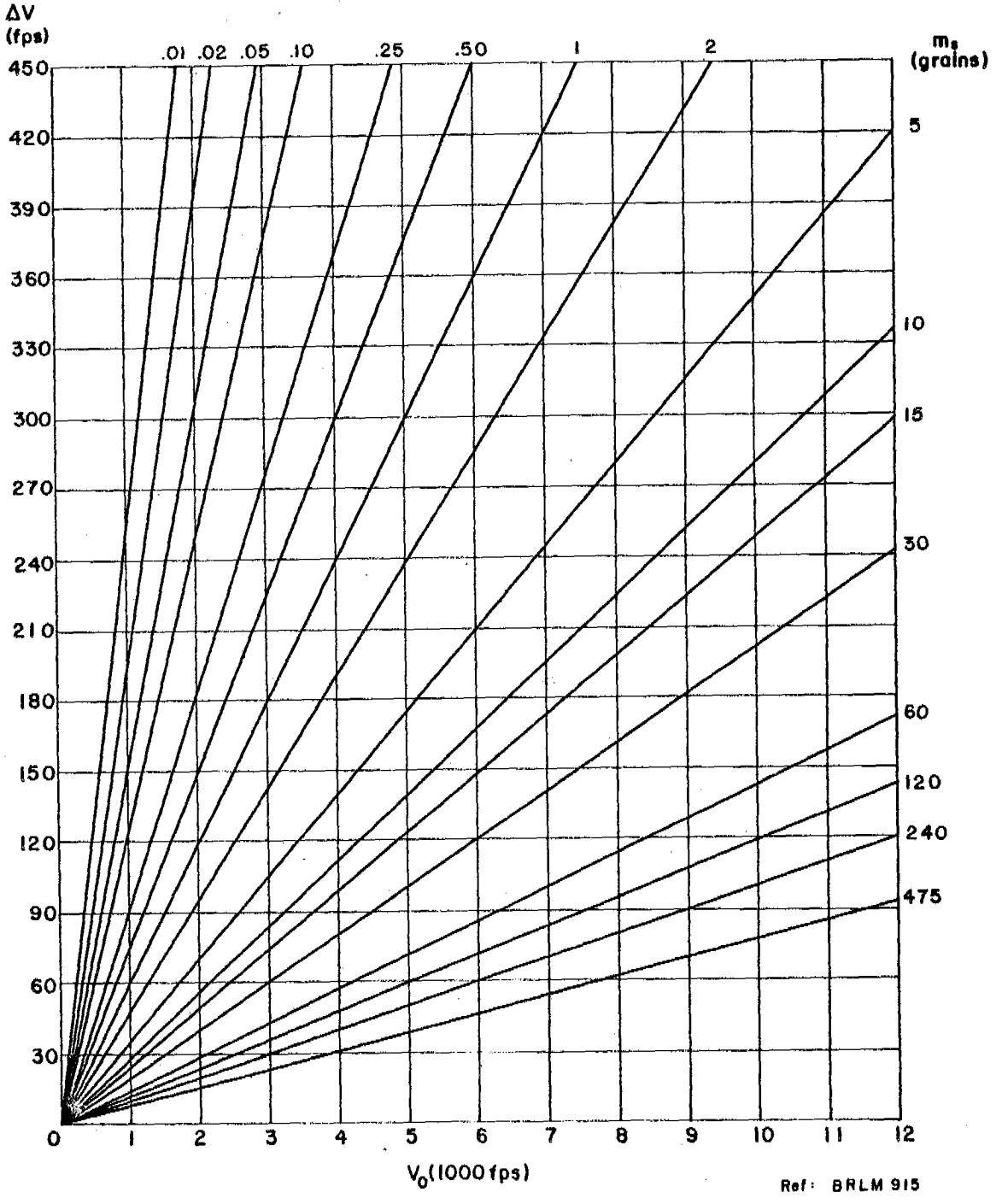


Fig. 19

## Retardation for Aluminum Alloy Fragments in Air

Notes:
a) Fragment has moved only one foot
b) Fragment moving at standard, sea-level conditions
c) $C_D \sim 0.56$

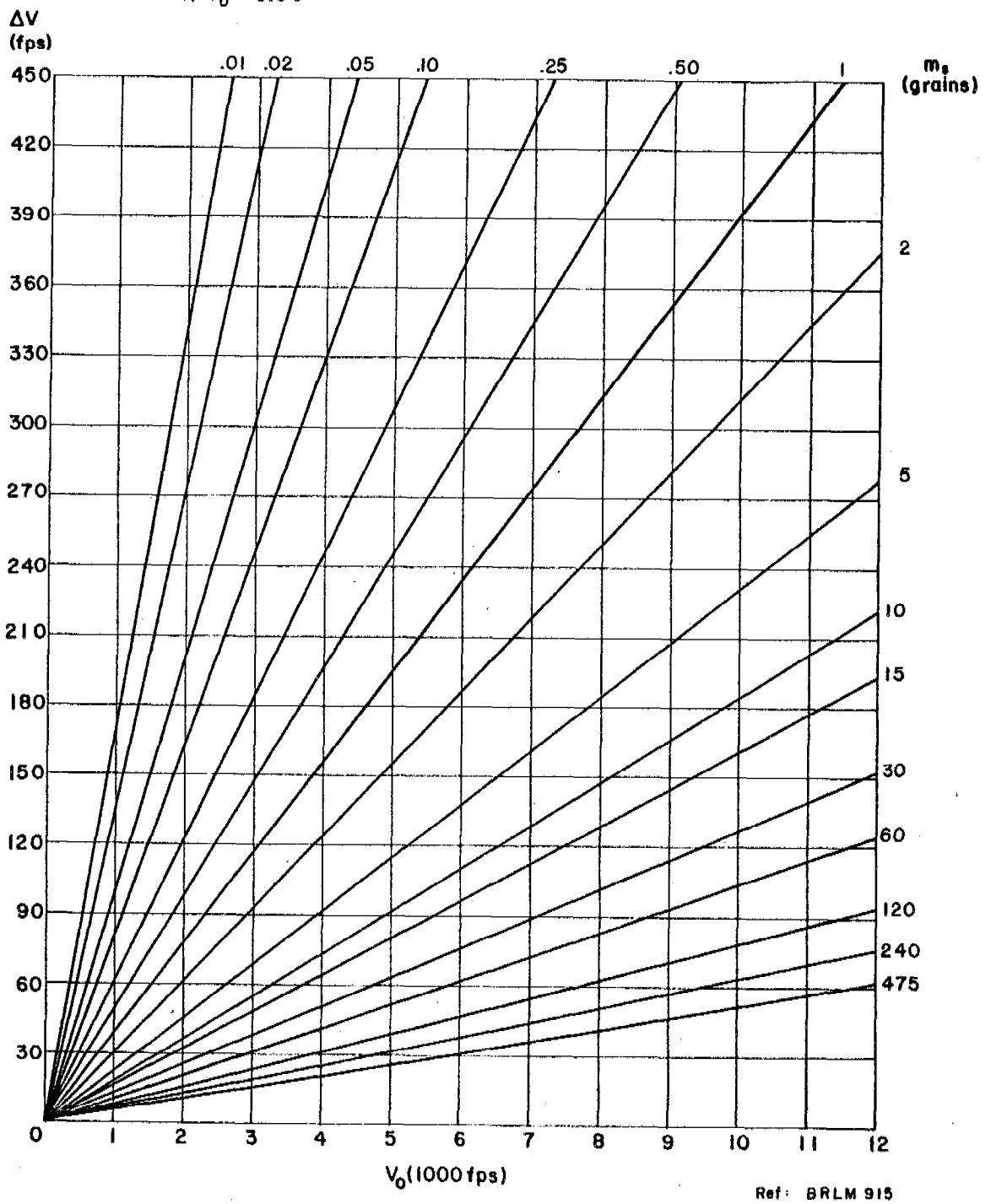


Fig. 20

## Retardation for Steel Fragments in Air

Notes:
a) Fragment has moved only one foot
b) Fragment moving at standard, sea-level conditions
c) $C_D \sim 0.56$

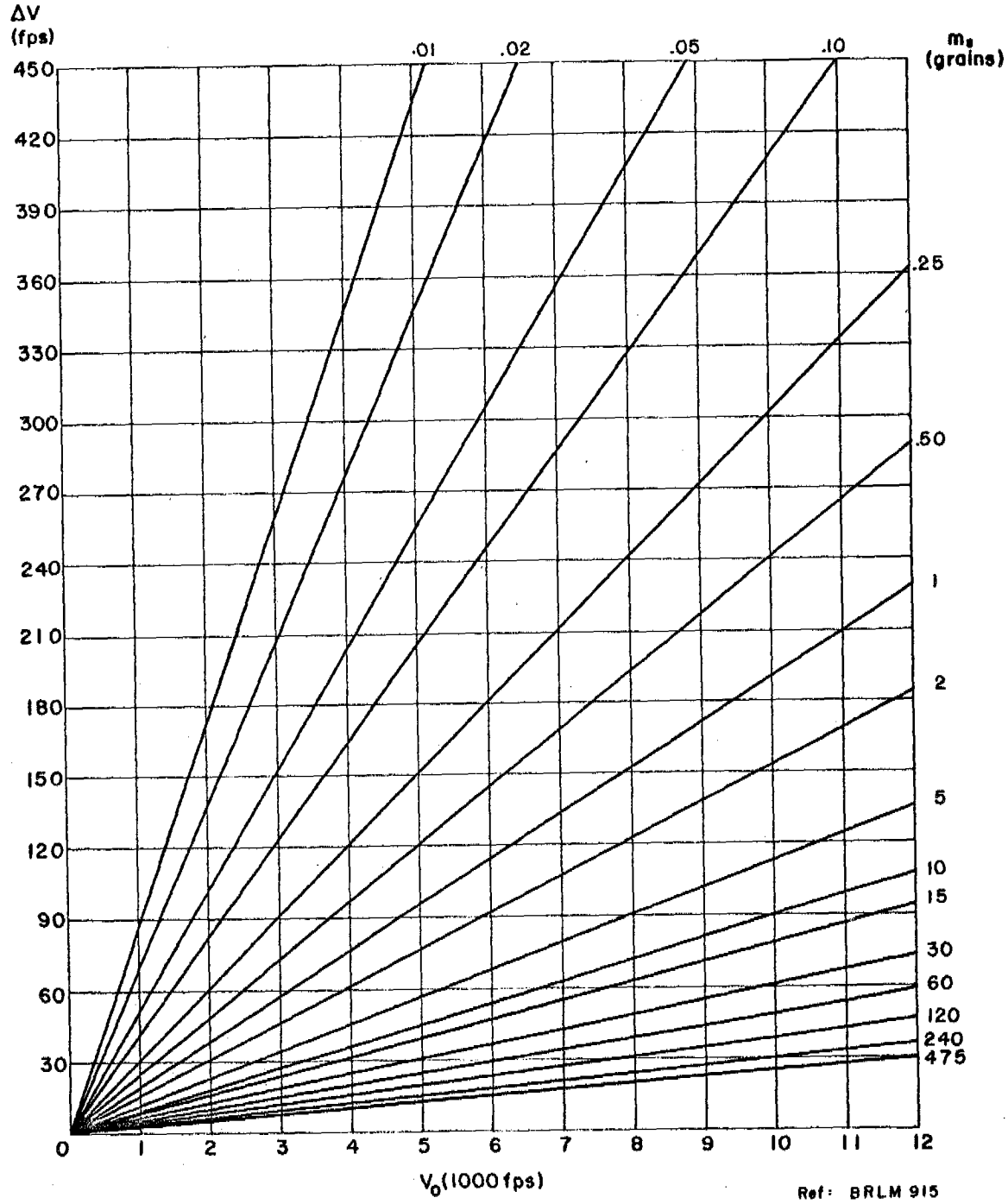


Fig. 21

## Retardation for Tungsten Alloy Fragments in Air

Notes:
a) Fragment has moved only one foot
b) Fragment moving at standard, sea-level conditions
c) $C_D \sim 0.56$

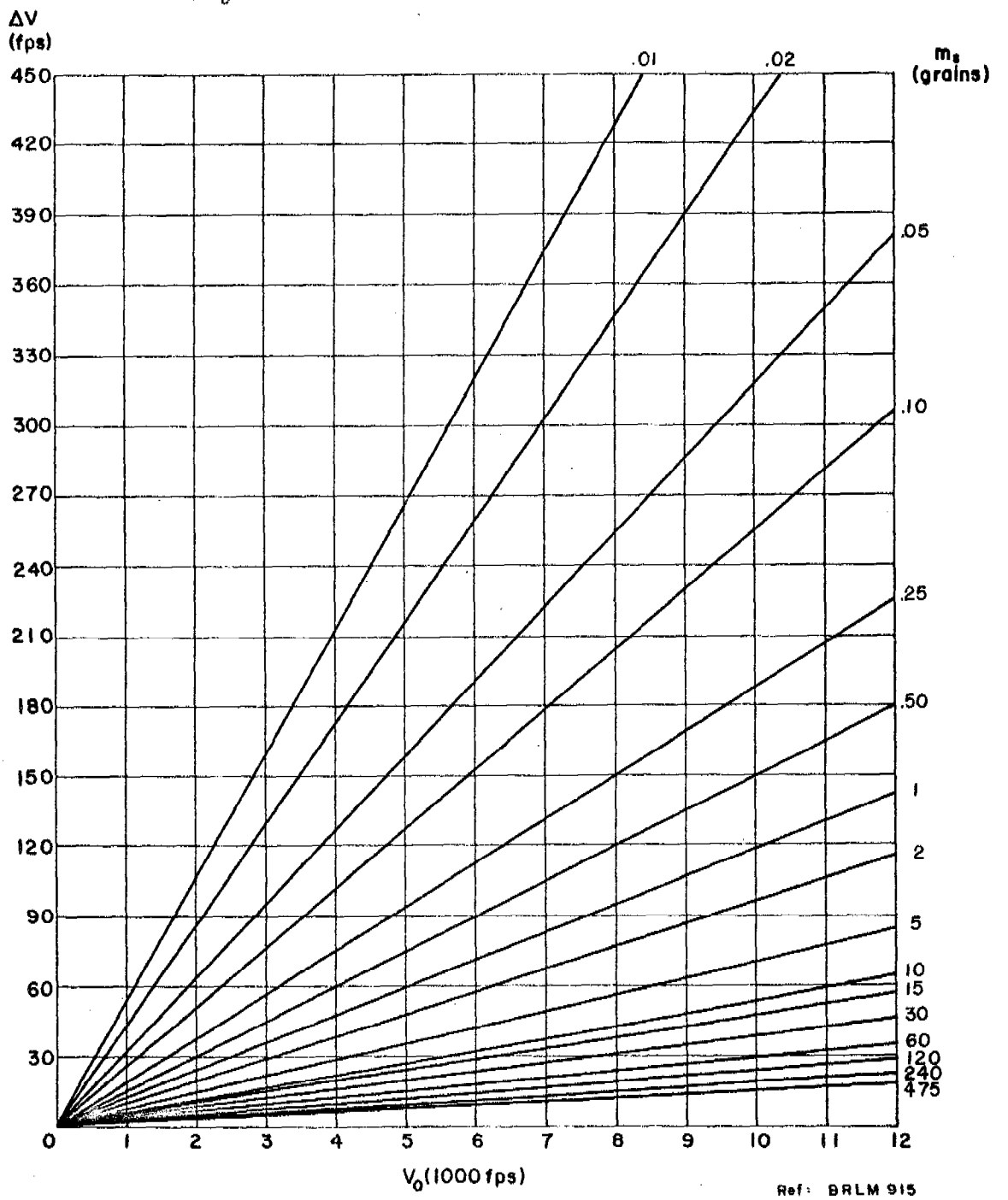


Fig. 22

This page intentionally blank

DISTRIBUTION LIST

| No. of Copies | Organization |
|---|---|
| 10 | Commander<br>Armed Services Technical Information Agency<br>ATTN: TIPCR<br>Arlington Hall Station<br>Arlington 12, Virginia |
| 1 | Commander<br>Field Command<br>Defense Atomic Support Agency<br>ATTN: FCDR/4<br>Sandia Base<br>P.O. Box 5100<br>Albuquerque, New Mexico |
| 6 | Chief of Ordnance<br>ATTN: ORDTB - Bal Sec<br>Department of the Army<br>Washington 25, D.C. |
| 4 | Commanding Officer<br>Picatinny Arsenal<br>ATTN: Mr. F. Saxe<br>Mr. J. Killen<br>Dr. N. Clarke<br>Dover New Jersey |
| 1 | Commanding General<br>Frankford Arsenal<br>ATTN: Mr. H. Markus<br>Philadelphia 37, Pennsylvania |
| 1 | Commanding Officer<br>Watertown Arsenal<br>ATTN: Watertown Arsenal Lab<br>Armor Section<br>Watertown 72, Massachusetts |
| 3 | Commanding General<br>U.S. Army Ordnance Missile Command<br>ATTN: Mr. P. Mullowney<br>Mr. C. Cockrell<br>Library Section<br>Redstone Arsenal, Alabama |
| 1 | Commanding Officer<br>Diamond Ordnance Fuze Laboratories<br>ATTN: Technical Information Office, Branch 012<br>Washington 25, D.C. |
| 1 | Commanding Officer<br>Ordnance Material Research Office<br>ATTN: Mr. B. Goldberg<br>Watertown Arsenal<br>Watertown 72, Massachusetts |
| 2 | Commanding General<br>Ordnance Tank-Automotive Command<br>ATTN: Mr. H. Spiro<br>Mr. Charles Saulter<br>1501 Beard Street<br>Detroit 9, Michigan |
| 2 | Commanding Officer<br>Philadelphia Ordnance District<br>ATTN: OD, R&D Branch<br>128 North Broad Street<br>Philadelphia, Pennsylvania |
| 1 | Commanding Officer<br>U.S. Army Chemical Center<br>ATTN: Mr. George Stewart<br>Army Chemical Center, Maryland |
| 2 | Commanding General<br>Quartermaster Research and Engineering Command<br>ATTN: Mr. A. Alessi<br>Natick, Massachusetts |
| 1 | Commandant<br>U.S. Army Artillery & Missile School<br>ATTN: Librarian<br>O. Willard Hollaway<br>Fort Sill, Oklahoma |

DISTRIBUTION LIST

| No. of Copies | Organization |
|---|---|
| 2 | Commanding General<br>Aberdeen Proving Ground, Maryland<br>ATTN: Technical Information Branch |
| 20 | Director<br>Ballistic Research Laboratories<br>ATTN: Weapon Systems Lab (5)<br>Terminal Ballistics Lab (5)<br>Reports Dist Sec (10)<br>Aberdeen Proving Ground, Maryland |
| 1 | Director<br>Development & Proof Services<br>ATTN: Mr. W.C. Pless<br>Aberdeen Proving Ground, Maryland |
| 1 | Commanding Officer<br>U.S. Naval Air Development Center<br>ATTN: WR-4<br>Johnsville, Pennsylvania |
| 1 | Commanding Officer<br>Naval Ordnance Laboratory<br>ATTN: Fuze Department<br>Corona, California |
| 1 | Commander<br>Naval Ordnance Laboratory<br>White Oak<br>Silver Spring 19, Maryland |
| 2 | Commanding Officer<br>U.S. Naval Ordnance Test Station<br>ATTN: Code 12, Mr. Naufeld<br>Code 4057, Mr. Zeitlin<br>China Lake, California |
| 10 | Director<br>U.S. Naval Research Laboratory<br>ATTN: Mr. W.W. Atkins<br>Washington 25, D.C. |
| 3 | Commander<br>U.S. Naval Weapons Laboratory<br>ATTN: Dr. A.V. Hershey<br>KBT-3S<br>Code W4-1; Missile Safety Staff<br>Dahlgren, Virginia |
| 2 | Commander<br>Air Proving Ground Center<br>ATTN: PGRE<br>PGTZM<br>Eglin Air Force Base, Florida |
| 1 | Commander<br>Foreign Technology Division<br>Wright-Patterson Air Force Base<br>Ohio |
| 1 | Commander<br>Kirtland Air Force Base, New Mexico<br>ATTN: AF Space Weapons Center |
| 3 | Commanding Officer<br>Naval Nuclear Ordnance Evaluation Unit<br>ATTN: Code 40<br>Kirtland Air Force Base, New Mexico |
| 2 | Air Force Ballistic Missile Division<br>ATTN: Capt Eibling (BSRVP) (1)<br>A.F. Unit Post Office<br>Los Angeles 45, California |
| | Of Interest to:<br>Space Technology Laboratories, Inc.<br>ATTN: Dr. Morris Rosen (1)<br>Box 95001<br>Los Angeles 45, California |

DISTRIBUTION LIST

| No. of Copies | Organization |
|---|---|
| 1 | Director, Marshall Space Flight Center<br>ATTN: Library Section<br>Redstone Arsenal, Alabama |
| 2 | U.S. Atomic Energy Commission<br>Sandia Corporation<br>ATTN: W.F. Hartman, Div 126<br>F.J. Weibell, Div 1285<br>Sandia Base<br>Albuquerque, New Mexico |
| 2 | Aerojet General Corporation<br>ATTN: K.N. Krezenhagen<br>Ann R. Chase, Libr at Downey, California<br>Azusa, California |
| 1 | Aircraft Armaments, Inc.<br>P.O. Box 126<br>Cockeysville, Maryland |
| 1 | Armour Research Foundation<br>ATTN: Librarian of Documents<br>33rd & Dearborn Streets<br>Chicago, Illinois |
| 2 | Boeing Airplane Company<br>ATTN: Ray M. Elam<br>Mail Stop 21-31<br>P.O. Box 3707<br>Seattle 24, Washington |
| 1 | Institute for Cooperative Research<br>The Johns Hopkins University<br>ATTN: H.R. Warfield, Dir<br>34th & Charles Streets<br>Baltimore 18, Maryland |
| 1 | University of Denver<br>Industrial Research Institute<br>ATTN: Mr. L.E. Smith<br>Denver 10, Colorado |
| 1 | University of Utah<br>ATTN: Explosives Research Group<br>Salt Lake City, Utah |
| 6 | The Scientific Information Officer<br>Defence Research Staff<br>British Embassy<br>3100 Massachusetts Avenue, N.W.<br>Washington 8, D.C. |
| 5 | Defence Research Member<br>Canadian Joint Staff<br>2450 Massachusetts Avenue, N.W.<br>Washington 8, D.C. |
| | 1 Copy of Interest to:<br><br>ORDTP - Major D.R. Balfour<br>Canadian Liaison Office |